Late Ordovician (post-Sardic) rifting branches in the North Gondwanan Montagne Noire and Mouthoumet massifs of southern France

J. Javier Álvaro, Jorge Colmenar, Eric Monceret, André Pouclet, Daniel Vizcaïno

Late Ordovician (post–Sardic) rifting branches in the North Gondwanan Montagne Noire and Mouthoumet massifs of southern France

J. Javier Álvaro[1]*, Jorge Colmenar[2], Eric Monceret[3], André Pouclet[4] and Daniel Vizcaïno[5]

[1] *Instituto de Geociencias (CSIC-UCM), c/ José Antonio Novais 12, 28040 Madrid, Spain, jj.alvaro@csic.es*

[2] *Geological Museum, Natural History Museum of Denmark, University of Copenhagen, Øster Voldgade 5-7, 1350 Copenhagen, Denmark, colmenar@unizar.es*

[3] *18 rue des Pins, 11570 Cazilhac, France, eric.monceret@orange.fr*

[4] *3 rue des foulques, 85560 Longeville-sur-mer, France, andre.pouclet@sfr.fr*

[5] *7 Jean-Baptiste Chardin, Maquens, 11090 Carcassonne, France, daniel.vizcaino@wanadoo.fr*

* Corresponding author

Abstract

Upper Ordovician–Lower Devonian rocks of the Cabrières klippes (southern Montagne Noire) and the Mouthoumet massif in southern France rest paraconformably or with angular discordance on Cambrian–Lower Ordovician strata. Neither Middle–Ordovician volcanism nor associated metamorphism is recorded, and the subsequent Middle Ordovician stratigraphic gap is related to the Sardic phase. Upper Ordovician sedimentation started in the rifting branches of Cabrières and Mouthoumet with deposition of basaltic lava flows and lahar deposits (Roque de Bandies and Villerouge formations) of continental tholeiite signature (CT), indicative of continental fracturing.

The infill of both rifting branches followed with the onset of: (1) Katian (Ka1–Ka2) conglomerates and sandstones (Glauzy and Gascagne formations), which have yielded a new brachiopod assemblage representative of the *Svobodaina havliceki* Community; (2) Katian (Ka2–Ka4) limestones, marlstones and shales with carbonate nodules, reflecting development of bryozoan-echinoderm meadows with elements of the *Nicolella* Community (Gabian and Montjoi formations); and (3) the Hirnantian Marmairane Formation in the Mouthoumet massif that has yielded a rich and diverse fossil association representative of the pandemic Hirnantia Fauna. The sealing of the subaerial palaeorelief generated during the Sardic phase is related to Silurian and Early Devonian transgressions leading to onlapping patterns and the record of high-angle discordances.

Highlights

A stratigraphic revision of the Upper Ordovician from the Montagne Noire and Mouthoumet is made.

Volcanism, unconformably overlying the Sardic gap, point to continental tholeiitic signature

Continental fracturing controlled the onset of rift branches postdating the Sardic phase

Sealing of the subaerial Sardic palaeorelief is related to Silurian and Devonian transgressions

Keywords: brachiopods, trilobites, stratigraphy, continental tholeiite, unconformity, diamictite.

1. Introduction

The so-called Sardic Phase was originally described in SW Sardinia (Stille, 1939) as an "early Caledonian" structural event characterized by an angular unconformity associated with metallogenic emplacement of ore deposits, E-W-trending faulting and mild folding. After Mid–Ordovician emergence and erosion, sedimentation was renewed with the record of the alluvial to fluvio-lacustrine Puddinga Beds (Barca et al., 1986; Martini et al., 1991; Caron et al., 1997). In contrast, central-northern Sardinia is characterized by the emplacement of a Middle Ordovician, sub-alkalic calc-alkalic volcanic suite, constrained between Arenig and Caradoc metasediments and dated at 465.4 ± 1.4 Ma by U–Pb methods (Oggiano et al., 2010). This geodynamic contrast in Sardinia has argued in favour of several interpretations, such as (1) the development of Mid–Ordovician intracratonic rifting, controlled by extensional tectonics coeval with compressional tectonics in SW Sardinia (e.g., Minzoni, 2011), and (2) the emplacement of an Andean-type arc (e.g., Oggiano et al., 2010). In any case, a relative agreement exists on the interpretation of an alkaline volcanic activity encased across the Ordovician–Silurian transition. Volcanic products are associated with Hirnantian glacial diamictites, and interpreted as the onset of rifting pulses (subsequent to the Sardic Phase) responsible for deposition of 'puddinga' beds and drastic variations in thickness (Lehman, 1975; Ricci and Sabatini, 1978; Leone et al., 1991; Helbing and Tiepolo, 2005).

Similar discussions about the geodynamic interpretation of laterally equivalent Sardic unconformities (interpreted as both orogenic subduction and transpressive-transtensive modifications of the Rheic Ocean opening patterns) were subsequently reported in eastern Pyrenees (Delaperrière and Soliva, 1992; Casas and Fernández, 2007; Casas, 2010; Casas et al., 2010, 2014; Navidad et al., 2010) and the Alps (Zurbriggen et al., 1997; Handy et al., 1999;

Guillot et al., 2002; Stampfli et al., 2002; Schaltegger et al., 2003; Franz and Romer, 2007; Zurbriggen, 2015).

The presence of pseudo–Caledonian deformation pulses, broad Middle–Ordovician gaps and associated volcanics was also reported in the Cabrières klippes of the southern Montagne Noire (Gèze, 1949; Boulange and Boyer, 1964; Gonord et al., 1964; Arthaud et al., 1976; Engel et al., 1980-81; Feist and Etchler, 1994) and in the Mouthoumet massif (von Gaertner, 1937; Durand-Delga and Gèze, 1956; Vila, 1965; Ovtracht, 1967; Cornet, 1980; Bessière and Schulze, 1984; Bessière and Baudelot, 1988; Bessière et al., 1989; Berger et al., 1990, 1993, 1997) (Figs. 1–2). However, their geodynamic interpretation was dramatically constrained by the lack of a detailed biochronologic control on the stratigraphic framework and geochemical information of their associated Upper Ordovician volcanic complexes. The aims of this paper are: (1) to diagnose the time-stratigraphic Mid–Ordovician (Sardic) gap in the Cabrières klippes of the southern Montagne Noire and its neighbouring Mouthoumet massif (North Gondwana); (2) to document a reviewed and updated lithostratigraphic framework for the Upper Ordovician (post–Sardic) volcanosedimentary complexes and strata, coupled with a new biostratigraphic sketch controlled by new brachiopod and trilobite assemblages; (3) to characterize the petrography and geochemistry of the associated magmatic activity; and (4) to place this multidisciplinary approach in a North-Gondwanan geodynamic context.

2. Geological background

The southern Montagne Noire represents the southernmost part of the French Massif Central. It consists of a framework of nappes and slices, marked in its southeastern edge by the so-called Cabrières klippes (Fig. 3). There, the Upper Ordovician partly infills the Carboniferous–Permian Gabian-Neffiès Basin (*sensu* Gèze, 1949), and forms the summits of the 'Grand Glauzy' and 'Roque de Bandies' hills, which give names to their homonymous lithostratigraphic units. The Upper Ordovician succession occurs as wild-flysch deposits with exotic blocks of various post–Cambrian ages emplaced by gravity slides (Engel et al., 1978, 1979; Feist and Echtler, 1994). Exposures of some of these olistolithic blocks allow reconstruction of a nearly complete Lower Ordovician succession including the St Chinian, Maurérie, Cluse de l'Orb and Landeyran formations (see Vizcaïno and Álvaro, 2001, 2003; Álvaro et al., 2014). Unconformably overlying the Lower Ordovician (Thoral, 1935; Gèze, 1949; Bérard, 1986), three lithostratigraphic units are differentiated, from bottom to top (Fig. 4): (1) volcaniclastic deposits associated with interstratified lava flows crosscut by rhyolitic dykes (Gonord et al., 1964), unnamed and with its upper contact broadly dated as Mid Ordovician by means of acritarchs (F. Martin, op. cit. *in* Nysæther et al., 2002); (2) the Katian (Ka1–Ka2; Caradoc) siliciclastic Glauzy Formation (Colmenar et al., 2013); and (3) the Katian (Ka2–Ka4;

Ashgill), mixed (carbonate-siliciclastic) Gabian Formation (Colmenar et al., 2013). The top of the Upper Ordovician is marked by an erosive unconformity that marks the base of Llandovery, graptolite-bearing, black shales, locally known as "tranche noire" (Centène and Sentou, 1975; Babin et al., 1988; Štorch and Feist, 2008).

The Mouthoumet massif lies south of Montagne Noire and north of the North Pyrenean frontal thrust (the latter *sensu* Laumonier, 2015). The massif contains four tectonostratigraphic units, from east (tectonically top) to west (bottom), the Serre de Quintillan, Félines-Palairac and Roc de Nitable thrust slices, and an unnamed parautochthon (Cornet, 1980; Bessière and Schulze, 1984; Bessière and Baudelot, 1988; Bessière et al., 1989; Berger et al., 1997) (Fig. 3). The Ordovician lithostratigraphic subdivision of Mouthoumet has been traditionally reported as informal lithological units compared to neighbouring formations from the southern Montagne Noire (Cabrières klippes) and eastern Pyrenees (e.g., Gèze, 1949; Bessière et al., 1989; Berger et al., 1997). As in the case of the Pyrenees and Montagne Noire, the Middle Ordovician is absent and its gap allows differentiation between a Lower Ordovician sedimentary sequence and an unconformably overlying Upper Ordovician–Devonian sedimentary package (Fig. 4). The Lower Ordovician consists of greenish and brownish shales and sandstones, dated to Tremadocian–'Arenig?' by acritarchs (Baudelot and Bessière, 1975, 1977; Cocchio, 1981, 1982; Berger, 1982). This siliciclastic unit contains interbedded thick flows (ca. 100 m) of porphyritic metarhyolites in the parautochthon, and metarhyolitic flows or sills overlain by metabasaltic flows in the lower part of the Serre de Quintillan slice and in the Davejean tectonic window, which had not yet been geochemically characterized (Bessière and Schulze, 1984; Bessière and Baudelot, 1988; Bessière et al., 1989; Berger et al., 1997). The hitherto poorly constrained stratigraphy of the area is updated and completed in the following section.

3. Stratigraphic framework

The Upper Ordovician of the Cabrières klippes and Mouthoumet massif, bracketed between the Sardic unconformity and the erosive unconformity that marks the base of Silurian black shales, comprises three formations in the Cabrières klippes and four formations in the Mouthoumet massif (Figs. 4–5). They are described below.

3.1. Cabrières klippes, southern Montagne Noire

3.1.1. Roque de Bandies Formation (new): it is up to 50 m and comprises, from bottom to top, polymictic breccia deposits, ranging from sand to boulder in size, overlain by lava flows and breccias interbedded with volcanosedimentary lenses (Gonord et al., 1964). Some rhyolitic dykes occur crosscutting the formation, but will not be described below. Its lower contact is an

erosive unconformity and its top is marked by the occurrence of volcanosedimentary conglomerates, which are included in the overlying Glauzy Formation.

Whole rock mafic lavas yielded $^{40}Ar/^{39}Ar$ ages ranging between 330 and 345 Ma, which informs about the resetting age of Variscan granitic intrusion associated with wild-flysch deposition (Nysæther et al., 2002). The same authors included a palaeomagnetic analysis for these levels of 68º +17/–15 locating the southern Montagne Noire in high southerly latitudes

3.1.2. Glauzy Formation (Colmenar et al., 2013), formerly known as 'Grès à *Trinucleus'* (Bergeron, 1889), 'Formation gréseuse' (Dreyfuss, 1948), 'Grès, poudingues et quartzites à *Calymenella Boisseli* et Bryozoaires' (Gèze, 1949), and 'Grès quartzitiques du Caradoc' (Gonord et al., 1964). The formation, up to 50 m thick, consists of basal volcanosedimentary (litharenitic) conglomerates and conglomerate/shale alternations, grading upsection into subarkoses and greywackes rich in quartzite pebbles, bioclastic lags marking the base and laminae of trough cross-stratified sets, and iron-oxydroxide cements, conspicuous as coatings and impregnations (Fig. 6A). Glaucarenites are locally abundant and display a mixture of detrital (polyphasic) and authigenic varieties of glauconite (Fig. 6B). The formation represents reworking of the underlying Roque de Bandies Formation, grading upsection into the onset of shoreface-dominated substrates. Brachiopods belonging to the *Svobodaina havliceki* Community (Colmenar et al., 2013), trilobites and cystoids yielded by sandstone sets point to a late Caradoc–early Ashgill age or Katian (Ka1–Ka2 stage slice *sensu* Bergström et al., 2009) (Havlíček, 1981; Colmenar et al., 2013).

Some basal shale interbeds have yielded a poorly preserved acritarch association with *Priscogalea striatula* (Vavrdová, 1966) and *Striatotheca principalis parva* Burmann, 1970 (F. Martin *op. cit.* Nysæther et al., 2002) of probable Mid–Ordovician (pre–Caradoc) age. However, the probable reworking of the Lower Ordovician acritarch-bearing basement (well constrained in the conglomerates and litharenites that characterize the Roque de Bandies/Glauzy transition) should be taken into consideration.

3.1.3. Gabian Formation (Colmenar et al., 2013) was formerly known as 'Schistes à *Orthis Actoniae* and calcaires à Cystidés' (Bergeron, 1889), 'Calcaires et marnes schisteuses' (Dreyfuss, 1948) and 'Calcaires en plaquettes et marnes schisteuses à *Orthis* (*Nicolella*) *Actoniae*, and Cystoïdes et Bryozoaires' (Gèze, 1949). The formation, 10–25 m thick, consists of floatstone-dominated limestones, marlstones and shales bearing carbonate nodules rich in bryozoans and cystoids, and subsidiary brachiopods and trilobites. It is representative of the *Nicolella* Community and dated as Katian (Ka2–Ka4 according to Bergström et al., 2009). The formation represents the development of bryozoan-echinoderm meadows similar to other "lower–middle Ashgill" carbonate-dominated units associated with the Boda event (for more

details, see Villas et al., 2002; Boucot et al., 2003; Fortey and Cocks, 2005). Its top is marked by a gap overlain by Llandovery graptolitic black shales.

3.2. Mouthoumet

The Upper Ordovician volcanosedimentary units of the Mouthoumet massif, bounded by the Middle Ordovician unconformity and the Silurian black shales, can be lithostratigraphically subdivided as follows:

3.2.1. Villerouge Formation (new): its outcrops are exposed in the vicinity of Villerouge-Termenès and cover part of the Lacamp Plateau and the Evêque Forest (Félines-Palairac slice). Its selected stratotype lies along the Marmairane creek (N43º00'14.13'', E02º40'07.28''), east of Villerouge-Termenès (Fig. 3). The formation is ca. 50 m thick and consists of lava flows and breccias, interbedded with variegated shales and subsidiary litharenites. The top of the formation is characterized by a distinct unit, about 4-8 m thick, composed of poorly sorted, gravel-to-boulder, highly weathered mafic and shaly fragments, subrounded to angular in shape, embedded in a heterolithic volcaniclastic matrix. Stratification is absent, bases are inversely graded and the fabric is dominantly matrix-supported (Fig. 6C). Silicification of clasts is pervasive. The presence of relic feldspar microlites and mafic clasts (Fig. 6D–E), altered and rich in iron oxyhydroxide cements, suggests the matrix was originally may have been tuffaceous. This unit is interpreted as volcanic subaerial pyroclastic and debris flows (lahars) where, the presence of conspicuous silicified clasts, indicates cannibalization of the Lower Ordovician, shale-dominated, basement. Some acidic interbeds and dykes are crosscutting the above-reported mafic assemblage, but they will be not described below. The base of the Villerouge Formation is marked by an erosive unconformity, and its top is marked by the volcaniclastic conglomeratic lag that forms the basal part of the overlying Gascagne Formation (see below). Durand-Delga and Gèze (1956) included this volcanic unit in the overlying Upper Ordovician–Silurian succession, whereas Berger et al. (1997) associated it with the Lower Ordovician acidic episodes of the area and mapped it with the same symbol (ρα). A radiometric age is necessary to solve this stratigraphic puzzle, although we consider them as capping the Sardic unconformity: both the Roque de Bandies and the Villerouge formations form the basal infill of the Upper Ordovician troughs recognized in Cabrières and Mouthoumet, their bases are erosive unconformities, and their volcaniclastic counterparts are exclusively recognized in the overlying Upper Ordovician strata.

3.2.2. Gascagne Formation (new): this fossiliferous sandstone-dominated unit ranges from about 100 m thick in Laroque de Fa (Serre de Quintillan slice) to 5 m thick in the Félines-

Palairac slice. It was previously known as 'Caradoc sandstones' and consists of basal volcaniclastic conglomerates and lags covered by litharenite-to-arkose lenses and beds with shale interbeds increasing in thickness upsection. Its stratotype lies at the homonymous hill (N42°57'19.39", E2°34'32.19"), east of Laroque de Fa.

The lower part of the formation, directly overlying the Villerouge Formation, consists of polymictic (volcaniclastic-dominated) conglomerates and breccias, reaching up to 8 m in thickness. Clast size ranges from sand to boulder. They are chaotically oriented and display a clast-supported texture (Fig. 6F). Only locally, they are supported in a shale matrix suggesting their local transport by debris flow.

A sampling in the upper sandstone/shale alternations of the formation in the Gascagne area has yielded, in order of abundance (Fig. 7A–I): the brachiopods *Portranella exornata*, *Kjaerina* (*K.*) *gondwanensis*, *Svobodaina*? sp., *Iberomena sardoa*, *Drabovia* sp., *Rostricellula termieri*, *Tafilaltia* sp., *Hirnantia* sp. and Strophomenidae indet; the trilobites *Calymenella* cf. *boisseli*, *Dalmanitina* sp., *Dreyfussina* sp. and *Onnia* sp.; and undetermined gastropods, "*Cornulites*" sp. and cystoid columnar plates. Considering the brachiopod assemblage, the upper (volcanosedimentary-free) part of the Gascagne Formation can be correlated with the Glauzy Formation of the Montagne Noire (Colmenar et al., 2013); the lower part of the Porto de Santa Ana Formation in Buçaco, Portugal; the uppermost beds of the "Bancos Mixtos" in Central Iberia (Villas, 1995), the upper half of the Fombuena Formation in the Iberian Chains, NE Spain (Villas, 1985); the Cava Formation of the Spanish Central Pyrenees (Gil-Peña et al., 2004); the base of the Portixeddu Formation in Sardinia (Leone et al., 1991); the Uggwa Shale Formation in the Carnic Alps, Austria (Havlíček et al., 1987); and the Upper Shale Member of the Bedinan Formation in Turkey (Villas et al., 1995). Based on these correlations and the dating of the basal part of the Porto de Santa Anna Formation in Portugal, dated as Pusgillian by means of chitinozoans (Paris, 1979, 1981) and acritarchs (Elaouad-Debbaj, 1978), the Gascagne Formation can be dated as Katian, Ka1–Ka2 stage slices (see Bergström et al., 2009).

3.2.3. Montjoi Formation (new): this fossiliferous mixed (carbonate-shale) unit was traditionally known as the Ashgill 'schistes troués' and 'limestone layers' and contains a rich and diversified shelly fauna of bryozoans, brachiopods and echinoderms. It is a shale-dominated unit, up to 90 m thick, which displays common limestone nodules parallel to stratification and lenticular beds, up to 1.4 m thick. The formation crops out in the parautochthon, where it unconformably overlies the above-reported Villerouge Formation. Its stratotype lies along the road D212, 1 km SW of Montjoi (N42º59'11.19'', E02º28'28.65'').

The Montjoi Formation, also representative of the development of bryozoan-echinoderm meadows in mid-latitude settings, has yielded a rich echinoderm association, composed of *Aonodiscus spinosus*, *Caryocrinites crassus*, *C. elongatus*, *C. major*, *C. rugatus*,

Conspectocrinus celticus, Corylocrinus europaeus, Cyclocharax paucicrenellatus, Heliocrinites helmackeri, H. rouvillei, Mespilocystites cf. *lemenni, M.* cf. *tregervanicus, Ristnacrinus cirrifer* and *Trigonocyclicus* cf. *vajgatschensis* (Touzeau et al., 2012).

Associated with echinoderms and bryozoans, a new sampling has yielded gastropods and abundant brachiopods (Fig. 7J–M). Two new brachiopod associations have been identified: one at Montjoi-Le Moulin (association 1) and the other one at Termes (association 2). The former includes *Nicolella actoniae* and *Dolerorthis* sp.; and the latter *Kjaerina* (*Villasina*) sp., *Dolerorthis* sp. and Rafinesquinidae indet. The content of both associations, including some characteristic elements of the (brachiopod) *Nicolella* Community, allows a correlation with other Upper Ordovician Mediterranean bioclastic limestones and dolostones, such as the Gabian Formation in the Montagne Noire (Colmenar et al., 2013), the Uggwa Limestone and Wolayer formations from the Carnic Alps in Austria (Schönlaub, 1998), the Estana Formation in the Spanish Central Pyrenees (Gil-Peña et al., 2004), the Cystoid Limestone in the Iberian Chains (Villas, 1985), the Portixeddu and Domusnovas formations in Sardinia (Leone et al., 1991), the Rosan Formation in the Armorican Massif (Melou, 1987), the Upper Djeffara Formation in Libya (Buttler and Massa, 1996), and the upper part of the Porto de Santa Anna Formation in the Portuguese Central Iberian Zone (Colmenar, 2015). According to the correlation of Mediterranean formations bearing the *Nicolella* Community with the Pushgillian–to–Rawtheyan stages of the British scale (for a discussion, see Villas et al., 2002: fig. 1), the Montjoi Formation can be dated as Katian, stage slices Ka2–Ka4.

3.2.4. Marmairane Formation (new): although the above-reported Ashgill 'schistes troués' were traditionally described and mapped as directly overlain by Silurian black shales, in some areas yielding graptolites of the Llandovery–Wenlock transition (Ovtracht, 1967; Centène and Sentou, 1975; Berger et al., 1997), the lower part of these supposed 'Silurian black shales' is in fact represented by another distinct shaly unit. This new formation, up to 10 m thick, consists of green shales with rare dolostone nodules and centimetric sandy interbeds. In the parautochthon, this unit becomes a diamictite (unsorted sandy shale with hematite cement). Its name derives from a creek linking the Lacamp plateau and the Evêque Forest (Fig. 3). The new formation conformably overlies the Montjoi Formation in the parautochthon, and is either conformably or paraconformably overlain by the Silurian black shales in the parautochthon and the Félines-Palairac slice. Its stratotype lies along the homonymous creek (N43°0'2.38", E2°40'8.91").

In the parautochthon, some diamictitic beds are exposed along the road D212. They are formed by unsorted, sandy channel bodies that incised erosively into the underlying Montjoi Formation (Fig. 6G). Fossils have not been found in this bed and hence its age is constrained by lithostratigraphic correlation with laterally equivalent deposits of the Marmairane Formation.

The diamictite-free, offshore-dominated shales of the Marmairane Formation have yielded a new Hirnantian fauna of brachiopods and trilobites (Fig. 8). Five associations have been identified, four from Villerouge-Termenès (associations 1-4) and one from Gascagne (association 5). They are listed below, being the brachiopods ordered in descending abundance in each association: (1) Association 1 comprises *Hindella crassa incipiens*, *Plectothyrella crassicosta* ssp. and Dalmanellidae indet.; (2) Association 2 includes the brachiopods *Leptaena trifidum*, *Eostropheodonta hirnantensis*, Platyorthidae indet., *Glyptorthis* sp., Dalmanellidae indet, *Plectothyrella crassicosta* ssp., *Paucicrura* sp., *Rostricellula*? sp., *Orbiculoidea*? sp. and Orthidae indet; the trilobites *Dalmanitina* sp., *Flexycalymene* sp. and *Lichas* sp.; and undeterminated gastropods, dacryoconarids, and massive and ramose bryozoans; (3) Association 3 is represented by the brachiopods *Paucicrura* sp., Dalmanellidae indet, *Plectothyrella crassicosta* ssp. *Leptaena trifidum, Eostropheodonta* sp., Orthidae indet and *Orbiculoidea*? sp.; the trilobites *Flexycalymene* sp. and Dalmanitidae gen. et sp. indet.; and undeterminated gastropods; dacryoconarids, and massive and ramose bryozoans; (4) Association 4 includes the brachiopods *Hindella crassa incipiens*, *Leptaena trifidum*, *Eostropheodonta* sp., Dalmanellidae indet, *Leangella* sp. and *Plectothyrella*? sp.; the trilobite *Flexycalymene* sp.; and undeterminated gastropods, dacryoconarids, and massive and ramose bryozoans; and (5) Association 5 comprises the brachiopods *Kinnella kielanae* (very abundant), *Hirnantia sagittifera, Eostropheodonta* sp., Dalmanellidae indet., *Dalmanella testudinaria*, *Plectothyrella crassicosta* ssp. *Hindella crassa incipiens, Leptaena trifidum*, *Drabovinella* sp., *Destombesium*? sp. and *Howellites*? sp.; the trilobite *Mucronaspis* cf. *mucronata*, and undetermined crinoid columnar plates and ramose bryozoans. The fifth association occurs in homogeneous black-to-grey shales representative of lower offshore clayey substrates, whereas the former ones were yielded by green shales with centimetre-thick sandy tempestitic interbeds and scattered carbonate nodules reflecting upper offshore clayey-dominated substrates.

Most of the recorded brachiopods are typical elements of the Hirnantia Fauna (Temple, 1965; Rong and Harper, 1988), such as *Hirnantia sagittifera, Hindella crassa incipiens, Leptaena trifidum, Eostropheodonta hirnantensis, Dalmanella testudinaria* and *Plectothyrella crassicosta.* Based on this fossil content, the Marmairane formation can be correlated with classical Hirnantian formations, such as the Hirnant Formation in Wales (Temple, 1965), the Kosov Formation in Bohemia (Marek and Havlíček, 1967), the Loka Formation from Sweden (Bergström, 1968), the Kuanyingchiao Beds (Rong, 1979) and the Langøyene Formation from Norway (Brenchley and Cocks, 1982), among others. Based on the correlation with the Hirnantia Fauna-bearing formations, the Marmairane formation can be dated as Hirnantian.

4. Volcanic products

The petrography and geochemistry of the Roque de Bandies and Villerouge formations are described separately.

4.1. Roque de Bandies Formation, Cabrières klippes

The volcanic activity of the Roque de Bandies Formation is located in its lower part and consists of lava and volcaniclastic flows and tephra deposits interbedded with volcanosedimentary sequences. The lava composition shows dominantly mafic products. Crosscutting rhyolitic dykes are not considered here.

The mafic lavas are hyalo-microlitic with abundant and large phenocrysts of feldspar, phenocrysts of a ferro-magnesian mineral replaced by ferric hydroxide that could be a pyroxene due to its crystal shape, and microphenocrysts of magnetite. The groundmass is rich in plagioclase microliths and ferro-magnesian and oxide microcrysts. It is highly invaded by secondary quartz, calcite and ferric hydroxides. Subrounded and disaggregated xenoliths of crustal felsic rocks are common. Weathering alteration is widespread. Consequently, the sampling is hazardous and many analytical results have to be discarded.

Based on available analyses (Table 1), the chemical composition is basaltic and mafic to moderately evolved ($53.1 < SiO_2$ wt% < 58.4; $1.1 < TiO_2 < 1.3$; $6.2 <$ total $Fe_2O_3 < 11.6$; $1.9 < MgO < 1.9$; $3.1 < Na_2O < 4.1$; $0.9 < K_2O < 1.0$). The MgO content is anomalously low considering the amount of altered former pyroxenes. The loss on ignition is high (6.4 –7.7). Consequently, the magnesia and alkali contents have no significance and the CIPW norm calculation is unavailing. Indeed, the abundance of plagioclase phenocrysts and the crystallization of plagioclase before pyroxene are consistent with a tholeiitic magma. Moreover, the dark colouring of the groundmass during alteration indicates high iron content of the matrix, which is characteristic of a ferro-tholeiite, the first evolved term of the tholeiitic series. In return, the incompatible trace element abundances seem to be relatively well preserved. The rare earth elements are enriched and fractionated ($34.4 < La < 37.7$; $8.0 < La/Yb < 10.3$; $5.8 <$ chondrite normalized $La/Yb_{NC} < 7.4$) with no significant Eu-anomaly. The N-MORB normalized patterns (Fig. 9A) are characterized by enrichment of the most incompatible lithophile elements ($4.0 < Th/La_{NM} < 4.8$; $3.8 < Rb/La_{NM} < 5.1$; $3.3 < Ba/La_{NM} < 4.4$), Nb and Ta negative anomalies ($0.44 < Nb/La_{NM} < 0.50$; $0.43 < Ta/La_{NM} < 0.50$) and Ti negative anomaly ($0.36 < Ti/Ti^* < 0.45$) that may be partly a magmatic feature and the result of oxide fractionation. Compared to the CT average composition (Holm, 1985), the lavas can be defined as continental tholeiites, also shown by the Ti-Nb-Th ratios (Fig. 9B). In the Ta/Yb vs. Th/Yb diagram, the mantle source cannot be well defined because a part of the Th (and U) enrichment (Fig. 9A) may be due to crustal contamination due to the felsic xenoliths corresponding to the

UCC composition (Rudnick and Gao, 2004) (Fig. 9C). However, a moderately enriched source can be assumed.

4.2. Villerouge Formation, Félines-Palairac slice

The Villerouge Formation is dominated by mafic lava and pyroclastic flows and by laharic mudflows interbedded with shales. The mafic lavas display two petrographical types. The first type is hyalo-microlitic and highly phyric, rich in plagioclases with less abundant and sub-idiomorphic pyroxenes replaced by chlorite, and microphenocrysts of magnetite. The groundmass is rich in plagioclase microliths with undetermined ferro-magnesian and oxide microcrysts in an altered matrix of quartz, clay, calcite and ferric hydroxides. The second type is pilitic and less rich in phenocrysts, but includes glomeroporphyric aggregates of plagioclase. The groundmass is similar except the large size of microliths. In both types, xenoliths of quartz-feldspar aggregates and quartz-calcite veins are common. Weathering alteration is widespread and fresh samples are rather scarce.

Based on two analyses of the two types (Table 1), the chemical composition is basaltic and mafic to moderately evolved ($57.1 < SiO_2$ wt% < 58.3; $1.0 < TiO_2 < 1.2$; $7.8 <$ total $Fe_2O_3 < 9.1$; $1.8 < MgO < 2.4$; $4.6 < Na_2O < 5.2$; $1.1 < K_2O < 1.5$). The loss on ignition is moderate (3.5–3.6). The alteration effect seems to be low but a crustal contamination from sialic xenocrysts can be suspected. Meanwhile, the CIPW norm calculation displays an oversaturated tholeiitic composition. The abundance of plagioclase phenocrysts and the crystallization of plagioclase before pyroxene are consistent with a tholeiitic magma. The incompatible trace element abundances seem to be well preserved. The rare earth elements are enriched and fractionated ($21.4 < La < 32.9$; $7.6 < La/Yb < 10.4$; $5.2 <$ chondrite normalized $La/Yb_{NC} < 7.1$) with weak negative Eu-anomaly (0.7). The N-MORB normalized patterns (Fig. 9A) are characterized by enrichment of the most incompatible lithophile elements ($6.1 < Th/La_{NM} < 6.9$; $7.6 < Rb/La_{NM} < 7.6$; $5.5 < Ba/La_{NM} < 8.0$), Nb and Ta negative anomalies ($0.47 < Nb/La_{NM} < 0.49$; $0.52 < Ta/La_{NM} < 0.53$) and Ti negative anomaly ($0.45 < Ti/Ti^* < 0.53$) that may be partly a magmatic feature and the result of oxide fractionation. Compared to the CT average composition (Holm, 1985) the lavas can be defined as continental tholeiites, also shown by the Ti-Nb-Th ratios (Fig. 9B) similarly with the Roque de Bandies lavas. In the Ta/Yb vs. Th/Yb diagram, the mantle source cannot be well defined because a part of the Th (and U) enrichment (Fig. 9A) may be due to crustal contamination due to the felsic xenoliths corresponding to the UCC composition (Rudnick and Gao, 2004) (Fig. 9C), though a moderately enriched source can be assumed. This magmatic composition is close to that of both the Upper Ordovician Roque de Bandies lavas in the Cabrières klippes.

5. Mid–Ordovician gap and associated unconformities

In the Montagne Noire and Mouthoumet massifs, the age of the strata underlying the Sardic unconformity is highly variable, and ranges from the lower Cambrian Lastours Formation (Fournes slice) to the Lower Ordovician Landeyran Formation and "Lower Ordovician shales" (Cabrières klippes and Mouthoumet, respectively; Fig. 4). This stratigraphic relationship indicates the onset of a pronounced pre–Katian uplifted palaeorelief, which is deduced to be essentially fault-generated (paraconformable contacts with the Upper Ordovician are dominant, despite some significant high-angular discordances with Devonian strata; Fig. 6H). The minimum accumulative vertical displacement approached ca. 2 km (thickness of eroded formations, based on Álvaro et al., 1998; Vizcaïno and Álvaro, 2001, 2003).

After the Sardic uplift (responsible for generation of a pre–Katian paleorelief), extensional events appear to have caused rapid subsidence and collapse along the Cabrières and Mouthoumet troughs (or rifting branches), providing accommodation space for transgressive marine sedimentation. The tectonostratigraphic distribution of Upper Ordovician rocks suggests a peak of extensional tectonic activity just preceding the effusion of the lava flows that form the Roque de Bandies and Villerouge formations. The post–Sardic sedimentary succession starts with polygenic heterometric conglomerates and breccias, up to 60 m thick, which mark the base of the Ka1–Ka2 (upper Caradoc–lower Ashgill) Glauzy and Gascagne formations. Their clasts were derived from both the underlying Roque de Bandies and Villerouge formations, and from the Cambrian–Lower Ordovician succession that form the pre–Sardic basement.

Adjacent still rifting shoulders remained under subaerial exposure and erosion. Progressive onset of marine sedimentation was diachronous and controlled by subsidence and onlapping patterns, beginning in the early Katian in the Cabrières klippes and Mouthoumet, with progressive younger strata of Silurian (Fournes and Minervois nappes) and Devonian (Mt Peyroux and Pardailhan nappes; see their relative setting in Figs. 1–2). A petrographic analysis of the Lochkovian "mur quartzeux" (*sensu* Thoral, 1935) in the Mt Peyroux nappe (Feist and Schönlaub, 1973; Quémart et al., 1993) has pointed out the wealth in metamorphic (e.g., almandine) and anatectic and volcanic zircons, reflecting the emersion of a complex source area, different to that recognized in the Lower Ordovician (Dabard and Chauvel, 1991).

At least, another major gap is recognized in the study area related to the Gabian/Silurian black shales contact in Cabrières and the Gascagne/Marmairane contact in Mouthoumet, which can be interpreted as the onset of the Hirnantian glaciogenic erosion. Another apparent gap, marking the Villerouge/Montjoi contact may be related to Variscan faults and lack of adequate exposures. Finally, Silurian sea-level rise was likely caused by a combination of increased rates of tectonic subsidence and eustatic rise.

6. Palaeogeographic and geodynamic implications

The superposition of the Variscan and Alpine deformation in SW Europe has led to the onset of a complex puzzle of tectonostratigraphic units, which will still be during next decade a matter of debate. The suspected location of Iberia during Early Palaeozoic times should be replaced by assuming: (1) a 100–250 km right lateral offset along the North-Pyrenean fault system and the left lateral motion along the Sillon Houiller (or Villefranche) Fault (e.g., Choukroune and Mattauer, 1978; Raymond, 1987; Rosenbaum et al., 2002; Tugend et al., 2015; among others); and (2) a 35° clockwise rotation for cancelling the Gulf of Biscay (or Gulf of Gascogne) opening (Perroud and Bonhommet, 1981; Sibuet et al., 2004). The Mouthoumet massif is considered as the southern prolongation of the southern Montagne Noire. As a result, after counter-folding the Variscan Ibero-Armorican Arc, its northeastern branch would show a Gondwanan margin linking laterally, according to present coordinates, (1) the Pyrenean and South-Armorican Domains to the west, and (2) the Montagne Noire-Mouthoumet-Albigeois-Cévennes units and their Sardinia-Corsica prolongation to the east. The Sardic phase offers some distinct characters throughout the NE branch of the Ibero-Armorican branch.

Sardinia, where the 'phase' was originally defined, is traditionally subdivided into three tectonostratigraphic units that display different Sardic records. In SW Sardinia, the Cambrian–Lower Ordovician basement was deformed in W-E-trending open folds during the Mid Ordovician (Barca et al., 1986) Sardic Phase. By contrast, central Sardinia was protected from deformation, and its Middle Ordovician is characterized by the effusion of abundant acidic and basic submarine and subaerial volcanics (Memmi et al., 1983). In the northernmost nappes of Sardinia, the Middle–Upper Ordovician succession consists of thick turbidites and submarine volcanics that may reach 1–1.5 km in thickness (Funedda and Oggiano, 2009). As a result, the Middle Ordovician tectonic patterns recorded a distinct inversion from compressive to extensive tectonics toward the present-day north. Whether metamorphism and significant deformation were associated with the Sardic phase is still a matter of debate: some authors reject the concept of a Sardic 'folding' phase and attribute the structuring exclusively to a Variscan overprint. By contrast, the abundance of Middle Ordovician calc-alkaline suites, made up of andesitic to dacitic and rhyolitic rocks, is interpreted by other authors, such as Di Pisa et al. (1992), Carmignani et al. (2001), Stampfli et al. (2002), Buzzi et al. (2007) and Funneda and Oggiano (2009), as the onset of a Mid Ordovician arc that developed on North Gondwana as a consequence of the subduction of oceanic crust under continental crust (Andean-type convergence).

The eastern Pyrenees exhibit a similar stratigraphic sketch. The basement of the Sardic unconformity is highly variable, ranging from the Ediacaran Canaveilles to the Cambrian–Lower Ordovician Jujols groups. The uppermost shales of the latter have yielded in the vicinity

of La Molina, southern Canigou massif, an acritarch assemblage dated as Furongian–Early Ordovician (Casas and Palacios, 2012). Overlying the Sardic paraconformity to angular discordance, associated with the onset of NW-SE to N-S-trending, metre-to to hectometre-scale folds lacking cleavage development or metamorphism, the Upper Ordovician succession comprises, in ascending order: (1) the polymictic and polymetric Rabassa conglomerates (probably Caradoc in age); (2) the upper Caradoc–lower Ashgill sandy and volcanosedimentary Cava Formation, (3) the mid Ashgill carbonate-bearing Estana Formation; and (4) the Hirnantian Ansovell shales and diamictites capped by the Bar Quartzite. The Sardic unconformity is traditionally interpreted as a result of uplift, tilting and erosion of the basement (e.g., García-Sansegundo et al., 2004), although the geodynamic interpretation (subduction vs transtensive-transpressive modification of the Rheic Ocean opening patterns) is also still a matter of dispute (Stampfli and Borel, 2002; von Raumer and Stampfli, 2008; Stampfli et al., 2013). Laterally to the Cava Formation, some volcanosedimentary suites occur, such as the Pierrefitte volcanosedimentary complex composed of alkaline metabasalts and basic tuffs (Calvet et al., 1988) and other calc-alkaline volcanics of intermediate to acid composition (Martí et al., 1986) interpreted as representative of an orogenic setting. Recently, Casas et al. (2010) dated a Late Ordovician (456–446 Ma) plutonic event that emplaced granitic and dioritic bodies into the pre–Sardic basement, which was coeval with synsedimentary normal fault development in Upper Ordovician rocks.

In Iberia, the topmost (Floian) Armorican Quartzite *s.s.* (Gutiérrez-Alonso et al., 2007; Shaw et al., 2012, 2014) is interpreted as the result of erosion of the rift shoulders flanking the Rheic Ocean opening. However, its base generally lies unconformably on a thick, folded, Neoproterozoic to Cambrian turbidite sequence (McDougall et al., 1987), which von Raumer et al. (2008, 2013, 2015) associated with the collision of Gondwana with the Qaidam arc, subsequently followed by the accretion of the Qilian block.

In the Alps, a mid–Ordovician compressive event was also reported by Zurbriggen et al. (1997) and Handy et al. (1999) in the Sesia area, where it is associated with amphibolite facies metamorphism, HP metamorphism in the Aar massif (468 Ma; Schaltegger et al., 2003) and in the southern Alps (457±5 Ma; Franz and Romer, 2007).

As reported above, the Montagne Noire and Mouthoumet massifs also display a Sardic unconformity, with a minimum Mid–Ordovician gap, which ended a distinct Early–Ordovician episode of high rift-related subsidence rate patterns (von Raumer and Stampfli, 2008: figure 3). Neither open folds, nor related volcanism/hydrothermalism/metamorphism have yet been associated with this unconformity. Although clearly erosive, this unconformity is dominantly paraconformable and, in the absence of other arguments, the erosive incision in some outcrops (reaching the lower Cambrian Lastours Formation in the Fournes nappe) and the angular

unconformities shown in some outcrops (e.g., in the Pardailhan and Mt. Peyroux nappes; Fig. 6H) may be interpreted as a result of uplift, tilting and erosion.

In the reduced areas of Cabrières and Mouthoumet, the sharp modifications in facies and thicknesses of their involved Upper Ordovician formations suggest drastic modifications in the amount of available accommodation space, which should be generated by fault-controlled subsidence throughout an inherited uplifted Sardic palaeorelief. Inheritance of faults from pre–Sardic basement cannot be invoked here because of strong Variscan overprint and, in the case of the Cabrières klippes, incorporation of supposed (half)-grabens in Carboniferous wild flysch.

As in SW Sardinia and the eastern Pyrenees, the Upper Ordovician exposures of the Cabrières klippes and the Mouhoumet massif also comprise a distinct influence of rifting conditions related to extensional conditions, development of grabens or half-grabens. After the record of conglomerates and breccias associated with tholeiitic volcanic emplacement, both reduced troughs exhibit the record of the traditional fossiliferous Katian 1–2 (upper Caradoc–lower Ashgill) sandstone-dominated strata, Katian 2–4 (lower–middle Ashgill) carbonate-bearing strata and Hirnantian diamictites and shales. Denudation of a Sardic palaeorelief induced detrital petrography, which gradually changed from polymictic (volcanosedimentary and basement-influenced) conglomeratic litharenites to monomictic subarkoses and greywackes (the latter *via* greywackization, where matrix is controlled by the postdepositional transformation of argillaceous and volcanic rock fragments). A reactivation of the fault-controlled troughs took place across the Ordovician–Silurian transition, as a result of which the record of Hirnantian quartzites (distinct in Iberian and Pyrenean outcrops) is absent in the Montagne Noire and Mouthoumet massifs; this erosive unconformity is again covered in a diachronous and onlapping way, by Silurian black shales. It was during Early Devonian times when the Sardic palaeorelief was finally onlapped, in a diachronous way throughout the rift shoulders, and sealed by marine sediments (Fig. 4). Finally, a broad Late Devonian compression, reflecting the beginning of the Variscan Orogeny, is recorded throughout the French Massif Central (Faure et al., 2008, 2014).

7. Conclusions

The Lower/Upper Ordovician contact of the Cabrières klippes and the Mouthoumet massif is one of the most magnificent and important erosive unconformities preserved in the Montagne Noire and Mouthoumet massifs. Here, the Upper Ordovician history is bracketed between the Sardic unconformity (ranging from paraconformable to angular discordant contacts) and a diachronous Silurian erosive unconformity, which marks the blanketing of an inherited palaeorelief by onlapping kerogenous black shales (Silurian) and conglomerates and sandstones (Devonian).

The Late Ordovician rifting event is illustrated by significant volcanic activity of continental tholeiitic lavas originated from melting of mantle and crust lithosphere. It led to fault-controlled subsidence and the generation of structurally controlled depocentres, at least in the Cabrières and Mouthoumet sectors of the Montagne Noire and Mouthoumet massifs in North Gondwana. It was accompanied by marine transgression and extensional pulses that gradually led to flooding and onlapping on the shoulders of the rifting branches that were finally sealed during Early Devonian times.

8. Acknowledgements

The authors thank the constructive remarks made by Josep Maria Casas (Barcelona) and Jürgen von Raumer (Friburg). Research was funded by projects CGL2010-39417, CGL2012-39471 and CGL2013-48877-P from Spanish MINECO.

9. References

Álvaro, J.J., Vizcaïno, D., Chauvel, J.J., Courjault-Radé, P., Dabard, M.P., Debrenne, F., Feist, R., Pillola, G.L., Vennin, E., 1998. Nouveau découpage stratigraphique des séries cambriennes des nappes de Pardailhan et du Minervois (versant sud de la Montagne Noire, France). Géol. France 1998 (2), 3–12.

Álvaro, J.J., Bauluz, B., Clausen, S., Devaere, L., Gil Imaz, A., Monceret, E., Vizcaïno, D., 2014. Stratigraphic review of the Cambrian–Lower Ordovician volcanosedimentary complexes from the northern Montagne Noire, France. Stratigraphy 11, 83–96.

Arthaud, F., Burg, J.P., Matte, P., 1976. L'évolution structurale hercynienne du massif de Mouthoumet (Sud de la France). Bull. Soc. géol. France (sér. 7) 18, 967–972.

Babin, C., Feist, R., Mélou, M., Paris, F., 1988. La limite Ordovicien–Silurien en France. In: Cocks, L.R.M., Rickards, R.B. (Eds.), A Global Analysis of the Ordovician–Silurian Boundary. Bull. Br. Mus. (Nat. Hist.) Geol. 43, 73–79.

Barca, S., Carmignani, L., Maxia, M., Oggiano, G., Pertusati, P.C., 1986. The Geology of Sarrabus. In: Carmignani, L., Cocozza, T., Ghezzo, C., Pertusati, P.C., Ricci, C.A. (Eds.), Guide-Book to the Excursion on the Paleozoic Basement of Sardinia. IGCP Newsl., Spec. Iss. 5, 51–60.

Baudelot, S., Bessière, G., 1975. Découverte d'acritarches d'âge Ordovicien inférieur dans le Massif de Mouthoumet (Aude). C. R. somm. Soc. géol. France, 171–173.

Baudelot, S., Bessière, G., 1977. Données palynostratigraphiques sur le Paleózoïque inférieur du massif de Mouthoumet (Hautes Corbières, Aude). Ann. Soc. géol. Nord 47, 21–25.

Bérard, P., 1986. Trilobites de l'Ordovicien inférieur des Monts de Cabrières (Montagne Noire – France). Mém. Centr. Et. Rech. Géol. Hydrol. Univ. Sci. Tech. (Montpellier II) 24, 1–220. CERGA, Montpellier.

Berger, G., 1982. Notice explicative de la feuille de Leucate à 1/50 000, no. 1979, BRGM, Orléans.

Berger, G., Boyer, F., Rey, J., 1990. Notice explicative de la feuille de Lézignan-Corbières à 1/50 000, no. 1038, BRGM, Orléans.

Berger, G., Boyer, F., Débat, P., Demange, M., Freytet, P., Marchal, J.P., Mazéas, H., Vantrelle, C., 1993. Notice explicative de la feuille de Carcassonne à 1/50 000, no. 1037, BRGM, Orléans.

Berger, G.M., Alabouvette, B., Bessière, G., Bilotte, M., Crochet, B., Dubar, M., Marchal, J.P., Tambareau, Y., Villatte, J., Viallard, P., 1997. Notice explicative de la feuille de Tuchan à 1/50 000, no. 1078. BRGM, Orléans.

Bergeron, J., 1889. Etude géologique du massif ancien situé au sud du "Plateau central". Ann. Sci. Géol. 22, 1–362.

Bergström, J., 1968. Some Ordovician and Silurian brachiopod assemblages. Lethaia 1, 23–27.

Bergström, S.M., Chen, X., Gutiérrez-Marco, J.C., Dronov, A., 2009. The new chronostratigraphic classification of the Ordovician System and its relations to major regional series and stages and to $\delta^{13}C$ chemostratigraphy. Lethaia 42, 97–107.

Bessière, G., 1987. Modèle d'évolution polyorogénique d'un massif hercynien: le massif de Mouthoumet (Pyrénées audoises). PhD, Toulouse Univ.

Bessière, G., Baudelot, S., 1988. Le Paléozoïque inférieur du massif de Mouthoumet (Aude, France) replacé dans le cadre du domaine sud-Varisque: révision et conséquences. C. R. Acad. Sci., Paris (sér. 2) 307, 771–777.

Bessière, G., Schulze, H., 1984. Le Massif de Mouthoumet (Aude, France): nouvelle définition des unités structurales et essai d'une reconstruction paléogéographique. Bull. Soc. géol. France 26, 885–894.

Bessière, G., Bilotte, M., Crochet, B., Peybernès, B., Tambereau, Y., Villatte, J., 1989. Notice explicative de la feuille de Quillan à 1/50 000, no. 1077. BRGM, Orléans.

Boucot, A.J., Rong, J.Y., Chen, X., Scotese, C.R., 2003. Pre–Hirnantian Ashgill climatically warm event in the Mediterranean region. Lethaia 36, 119–132.

Boulange, M.F., Boyer, F., 1964. Sur l'âge de la transgression post–Calédonienne dans le Sud de la Montagne Noire. C. R. Acad. Sci., Paris 259, 1309–1312.

Brenchley, P.J., Cocks, L.R.M., 1982. Ecological associations in a regressive sequence: the latest Ordovician of the Oslo-Asker district, Norway. Palaeontology 25, 783–815.

Burmann, G., 1970. Witere organische Mikrofossilien aus dem unteren Ordovizium. Paläontol. Abh., Abt. B 3, 289–332.

Buttler, C., Massa, D., 1996. Late Ordovician bryozoans from carbonate buildups, Tripolitania, Libya, p. 63–68. In: Gordon, D.P., Smith, A.M., Grant-Mackie, J.A. (Eds.), Bryozoans in Space and Time. Proceedings of the 10th International Bryozoology conference, Wellington, New Zealand, 1995. National Institute of Water and Atmospheric Research Ltd., Wellington.

Buzzi, L., Gaggero, L., Funedda, A., Oggiano, G., Tieplolo, M., 2007. Zircon geochronology and Sm–Nd isotopic study of the Ordovician magmatic event in the southern Variscides (Sardinia). Géol. France 2, 73.

Calvet, P., Lapierre, H., Chavet, J., 1988. Diversité du volcanisme Ordovicien dans la région de Pierrefitte (Hautes Pyrénées): rhyolites calco-alcalines et basaltes alcalins. C. R. Acad. Sci., Paris 307, 805–812.

Carmignani, L., Conti, P., Barca, S., Cerbai, N., Eltrudis, A., Funedda, A., Oggiano, G., Patta, E.D., Ulzega, A., Orrè, P., Pintus, C., 2001. Note illustrative del Foglio 459 – Muravera. Memorie descrittive della Carta geológica d'Italia 1:50.000, 140 p.

Caron, C., Lancelot, J., Omenetto, P., Orgeval, J.J., 1997. Role of the Sardic tectonic phase in the metallogenesis of SW Sardinia (Iglesiente): lead isotope evidence. Eur. J. Miner. 9, 1005–1016.

Casas, J.M., 2010. Ordovician deformations in the Pyrenees: new insights into the significance of pre–Variscan ("Sardic") tectonics. Geol. Mag. 147, 647–689.

Casas, J.M., Fernández, O., 2007. On the Upper Ordovician unconformity in the Pyrenees: New evidence from the La Cerdanya área. Geol. Acta 5, 193–198.

Casas, J.M., Palacios, T., 2012. First biostratigraphical constraints on the pre–Upper Ordovician sequences of the Pyrenees based on organic-walled microfossils. C. R. Geosci. 344, 50–56.

Casas, J.M., Castiñeiras, P., Navidad, M., Liesa, M., Carreras, J., 2010. New insights into the Late Ordovician magmatism in the Eastern Pyrenees: U–Pb SHRIMP zircon data from the Canigó massif. Gondwana Res. 17, 317–324.

Centène, A., Sentou, G., 1975. Graptolites et conodontes du Silurien des massifs du Midi Méditerranéen. PhD, USTL Montpellier.

Choukroune, P., Mattauer, M., 1978. Tectonique des plaques et Pyrénées: sur le fonctionnement de la faille transformante Nord-Pyrénéenne, comparaison avec les modèles actuels. Bull. Soc. géol. France (sér. 7) 20, 689–700.

Cocchio, A.M., 1981. Microflores des séries du Paléozoïque inférieur du massif de Mouthoumet (Corbières, Aude). Etude systématique et comparaison avec les séries des Pyrénées orientales et de la Montagne Noire. PhD, Univ. Toulouse.

Cocchio, A.M., 1982. Donnés nouvelles sur les acritarches du Trémadoc et de l'Arénig dans le Massif de Mouthoumet (Corbières, France). Rev. Micropaléont. 25, 26–39.

Colmenar, J. 2015. The arrival of brachiopods of the *Nicolella* Community to the Mediterranean margin of Gondwana during the Late Ordovician: palaeogeographical and palaeoecological implications. Palaeogeogr., Palaeoclimat., Palaeoecol. 428, 12–20.

Colmenar, J., Villas, E., Vizcaïno, D., 2013. Upper Ordovician brachiopods from the Montagne Noire (France): endemic Gondwanan predecessors of Prehirnantian low-latitude immigrants. Bull. Geosci. 88, 153–174.

Cornet, C., 1980. Genèse structurale des Corbières. Bull. Soc. géol. France (sér. 7) 22, 179–184.

Dabard, M.P., Chauvel, J.J., 1991. Les variations bathymétriques pendant l'Arénig inférieur dans la Montagne Noire (versant Sud, région de Saint-Chinian). Géol. France 1991 (1), 45–54.

Delaperrière, E., Soliva, J., 1992. Détermination d'un âge Ordovicien supérieur–Silurien des gneiss de Casemi (Massif du Canigou, Pyrénées Orientales) par la méthode d'évaporation du plomb sur monozircon. C. R. Acad. Sci., Paris 314, 345–350.

Di Pisa, A., Gattiglio, M., Oggiano, G., 1992. Pre–Hercynian magmatic activity in the nappe zone (internal and external) of Sardinia: evidence of two within plate basaltic cycles. In: Carmingnani, L., Sassi, F.P., (Eds.), Contributions to the Geology of Italy with Special Regard to the Paleozoic Basements. IGCP No. 276 Newsl., 107–116.

Dreyfuss, M., 1948. Contribution à l'étude géologique et paléontologique de l'Ordovicien supérieur de la Montagne Noire. Mém. Soc. géol. France (nouv. sér.) 27 (58), 1–63.

Durand-Delga, M., Gèze, B., 1956. Les venues éruptives ordoviciennes de la Camp, près de Félines-Termenès (massif de Mouthoumet, Aude). C. R. somm. Soc. géol. France, 268–272.

Elaouad-Debbaj, Z., 1978. Acritarches de l'Ordovicien supérieur du synclinal de Buçaco (Portugal). Systématique, biostratigraphie, intérêt paléogéographique. Bull. Soc. géol. miner. Bretagne C2, 1–101.

Engel, W., Feist, R., Franke, W., 1978. Synorogenic gravitational transport in the Carboniferous of the Montagne Noire (S France). Z. dtsch. Geol. Gess. 129, 461–472.

Engel, W., Feist, R., Franke, W., 1979. Carte géologique du flysch carbonifère entre le Mont Peyroux et Cabrières. Montagne Noire SE, Hérault (France) 1:25 000. In: Feist, R. (Ed.), GRECO no. 7 CNRS. Lab. Géol. Historique. USTL, Montpellier.

Engel, W., Feist, R., Franke, W., 1980–1981. Le Carbonifère anté–stéphanien de la Montagne Noire: rapport entre mise en place des nappes et sédimentation. Bull. BRGM (sér. 2), 1 (4), 341–389.

Faure, M., Ledru, P., Lardeaux, J.M., Matte, P., 2004. Paleozoic orogenies in the French Massif Central. A cross section from Béziers to Lyon. 32nd Int. Geol. Congress, Florence (Italy). Field-trip Guide Book, 40 p.

Faure, M., Be Mezeme, E., Cocherie, A., Rossi, P., Chemenda, A., Boutelier, D., 2008. Devonian geodynamic evolution of the Variscan Belt, insights from the French Massif Central and Massif Armoricain. Tectonics 27, TC2005, doi:10.1029/2007TC002115.

Faure, M., Cocherie, A., Gaché, J., Esnault, C., Guerrot, C., Rossi, P., Wei, L., Qiuli, L., 2014. Middle Carboniferous intracontinental subduction in the Outer Zone of the Variscan Belt (Montagne Noire Axial Zone, French Massif Central): multimethod geochronological approach of polyphase metamorphism. In: Schulmann, K., Martínez Catalán, J.R., Lardeaux, J.M., Janousek, V., Oggiano, G. (Eds.), The Variscan Orogeny: Extent, Timescale and the Formation of the European Crust. Geol Soc., London, Spec. Pub. 405, 289–311.

Feist, R., Etchler, H., 1994. The Massif Central: external zones, 291–297. In: Keppie, J. (Ed.), Pre–Mesozoic Geology of France and Related Areas. Springer, Berlin.

Feist, R., Schönlaub, H.P., 1973. Le passage Siluro–Dévonien dans la Montagne Noire orientale. C. R. Acad. Sci., Paris (sér. D) 276, 1267–1270.

Fortey, R.A., Cocks, L.R.M., 2005. Late Ordovician global warming – The Boda event. Geol. Soc. Am. Bull. 33, 405–408.

Franz, L., Romer, R.L., 2007. Caledonian high-pressure metamorphism in the Strona-Ceneri-Zone (Southern Alps of southern Switzerland and northern Italy). Swiss J. Geosci. 100, 457–467.

Funedda, A., Oggiano, G., 2009. Outline of the Variscan basement of Sardinia. In: Corradini, C., Ferretti, A., Štorch, P. (Eds.), The Silurian of Sardinia. Volume in Honour of Enrico Serpagli. Rend. Soc. Paleont. It. 3, 23–35.

Gaertner von, H., 1937. Montagne Noire und Mouthoumet als Teile des südwest europäischen Variskums. Abh. D. Ges. D. Wiss. Zu Göttingen, Math.-Phys., K1, H17, 260 p.

García-Sansegundo, J., Gavaldà, J., Alonso, J.L., 2004. Preuves de la discordance de l'Ordovicien supérieur dans la zone axiale des Pyrénées: exemple de dôme de la Garonne (Espagne, France). C. R. Geosci. 336, 1035–1040.

Gèze, B., 1949. Etude géologique de la Montagne Noire et des Cévennes méridionales. Mém. Soc. géol. France (nouv. sér.) 62, 1–215.

Gil-Peña, I., Barnolas, A., Villas, E., Sanz-López, J., 2004. El Ordovícico Superior de la Zona Axial, p. 247–249. In: Vera, J.A. (Ed.), Geología de España. SGE-IGME, Madrid.

Gonord, H., Ragot, J.P., Saugy, L., 1964. Observations lithostratigraphiques nouvelles sur la série de base (Ordovicien inférieur) des nappes de Cabrières, région de Gabian-Glauzy (Montagne Noire, Hérault). Bull. Soc. géol. France 7, 419–427.

Guillot, F., Schaltegger, U., Bertrand, J.M., Deloule, E., Baudin, T., 2002. Zircon U–Pb geochronology of Ordovician magmatism in the polycyclic Ruitor Massif (Internal W-Alps). Int. J. Earth Sci. 91, 964–978.

Gutiérrez-Alonso, G., Fernández-Suárez, J., Gutiérrez-Marco, J.C., Corfu, F., Murphy, J.B., Suárez, M., 2007. U–Pb depositional age for the upper Barrios Formation (Armorican Quartzite facies) in the Cantabrian zone of Iberia: implications for stratigraphic correlation and paleogeography. In: Linnemann, U., Nance, R.D., Kraft, P., Zulauf, G. (Eds.), The Evolution of the Rheic Ocean: From Avalonian–Cadomian Active Margin to Alleghenian–Variscan Collision. Geol. Soc. Am. Spec. Pap. 423, 287–296.

Handy, M.R., Franz, L., Heller, F., Janott, B., Zurbriggen, R., 1999. Multistage accretion and exhumation of the continental crust (Ivrea crustal section, Italy and Switzerland). Tectonics 18, 1154–1177.

Havlíček, V., 1981. Upper Ordovician brachiopods from the Montagne Noire. Palaeontogr., Abt. A 176, 1–34.

Havlíček, V., Kriz, J., Serpagli, E., 1987. Upper Ordovician brachiopod assemblages of the Carnic Alps, Middle Carinthia and Sardinia. Boll. Soc. Paleont. It. 25, 277–311.

Helbing, H., Tiepolo, M., 2005. Age determination of Ordovician magmatism in NE Sardinia and its bearing on Variscan basement evolution. J. Geol. Soc. London 162, 689–700.

Holm., P.E., 1985. The geochemical fingerprints of different tectono-magmatic environments using hygromagmatophile element abundance of tholeiitic basalts and basaltic andesites. Chem. Geol. 51, 303–323.

Laumonier, B., 2015. Les Pyrénées alpines sud-orientales (France, Espagne) – essai de synthèse. Rev. Géol. pyrén. 2 (1), 44 p.

Lehman, B., 1975. Stratabound polymetallic and F–Ba deposits of the Sarrabus-Gerrei region, SE Sardinia. IV report: Initial Variscan magmatism in SE Sardinia. N. Jb. Geol. Paläont., Mh. 1971, 460–470.

Leone, F., Hammann, W., Serpagli, E., Villas, E., 1991. Lithostratigraphic units and biostratigraphy of the post–Sardic Ordovician sequence in south-west Sardinia. Boll. Soc. Paleont. It. 30, 201–235.

Marek, L., Havlíček, V., 1967. The articulate brachiopods of the Kosov Formation (upper Ashgillian). Vest. Ústred. úst. geol. 42, 275–284

Martí, J., Muñoz, J.A., Vaquer, R., 1986. Les roches volcaniques de l'Ordovicien supérieur de la région de Ribes de Freser-Rocabruna (Pyrénées catalanes): caractères et signification. C. R. Acad. Sci., Paris 302, 1237–1242.

Martini, I.P., Tongiorgi, M., Oggiano, G., Cocozza, T., 1991. Ordovician alluvial fan to marine shelf transition in SW Sardinia, Western Mediterranean Sea: tectonically (“Sardic phase”) influenced clastic sedimentation. Sediment. Geol. 72, 97–115.

McDougall, N., Brenchley, P.J., Rebelo, J.A., Romano, M., 1987. Fans and fan deltas – precursors to the Armorican Quartzite (Ordovician) in western Iberia. Geol. Mag. 124, 347–359.

Melou, M., 1987. Découverte de *Hirnantia sagittifera* (M'Coy 1851) Orthida Brachiopoda dans l'Ordovicien supérieur (Ashgillien) de l'extrémité occidentale du Massif Armoricain. Geobios 20, 679–686.

Memmi, I., Barca, S., Carmignani, L., Cocozza, T., Elter, F., Franceschelli, M., Gattiglio, M., Chezzo, C., Minzoni, N., Naud, G., Pertusati, P.., Ricci, C.A., 1983. Further geochemical data on the pre–Hercynian igneous activities of Sardinia and on their geodynamic significance. IGCP 5 Newsl. 5, 87–91.

Minzoni, N., 2011. Transtensional tectonics played a key role during the Variscan cycle in the Sardinia-Corsica Massif. In: Schattner, U. (Ed.), New Frontiers in Tectonic Research – At the Midst of Plate Convergence. In Tech, Rijeka, Croatia.

Navidad, M., Casas, J.M., Castiñeiras, P., Barnolas, A., Fernández-Suárez, J., Liesa, M., Carreras, J., Gil-Peña, I., 2010. Geochemical characterization and isotopic age of the Caradocian magmatism from North-Eastern Iberian Peninsula: Insights from the Late Ordovician evolution of the northern Gondwana margin. Gondwana Res. 17, 325–337.

Nysæther, E., Torsvik, T.H., Feist R., Walder-Haug, H.J., Eide, E.A., 2002. Ordovician palaeogeography with new palaeomagnetic data from the Montagne Noire (Southern France). Earth Planet. Sci. Lett. 203, 329–341.

Oggiano, G., Gaggero, L., Funedda, A., Buzzi, L., Tiepolo, M., 2010. Multiple early Paleozoic volcanic events at the northern Gondwana margin: U–Pb age evidence from the Southern Variscan branch (Sardinia, Italy). Gondwana Res. 17, 44–58.

Ovtracht, A., 1967. Notice explicative de la feuille de Quillan à 1/80 000, no. 254, BRGM, Orléans.

Paris, F., 1979. Les chitinozoaires de la Formation de Louredo, Ordovicien supérieur du Synclinal de Buçaco (Portugal). Palaeontogr. Abt A 164, 24–51.

Paris, F., 1981. Les chitinozoaires dans le Paléozoïque du Sud-Ouest de l'Europe. Mém. Soc. géol. miner. Bretagne 26, 1–412.

Perroud, N., Bonhommet, N., 1981. Paleomagnetism of the ibero-armoricain arc and the Hercynian orogeny in Western Europe. Nature 292, 5822, 445–448.

Pouclet, A., Lee, J.S., Vidal, P., Cousens, B., Bellon, H., 1995. Cretaceous to Cenozoic volcanism in South Korea and in the Sea of Japan: magmatic constraints on the opening of the back-arc basin. In: Smellie, J.L. (Ed.), Volcanism Associated with Extension at Consuming Plate Margins. Geol. Soc., London, Spec. Pub. 81, 169–191.

Quémart, P., Dabard, M.P., Chauvel, J.J., Feist, R., 1993. La trangression éo–dévonienne sur le Paléozoïque ancien dans la nappe du Mont Peyroux (Montagne Noire, Hérault): signature pétrographique et implications géodynamiques. C. R. Acad. Sci., Paris (sér. 2) 317, 655–661.

Raumer von, J.F., Stampfli, G.M., 2008. The birth of the Rheic Ocean – early Palaeozoic subsidence patterns and tectonic plate scenarios. Tectonophysics 461, 9–20.

Raumer von, J.F., Bussy, F., Schaltegger, U., Schulz, B., Stampfli, G.M., 2013. Pre–Mesozoic Alpine basements – their place in the European Paleozoic framework. GSA Bull. 125, 89–108.

Raumer von, J.F., Stampfli, G.M., Arenas, R., Sánchez Martínez, S., 2015. Ediacaran to Cambrian oceanic rocks of the Gondwana margin and their tectonic interpretation. Int. J. Earth Sci. 104, 1107–1121.

Raymond, D., 1987. Le Dévonien et le Carbonifère inférieur du sud-ouest de la France (Pyrénées, Massif du Mouthoumet, Montagne Noire): sédimentation dans un bassin flexural en bordure sud de la chaîne de collision varisque. Geol. Rundsch. 76, 795–803.

Ricci, C.A., Sabatini, G., 1978. Petrogenetic affinity and geodynamic significance of metabasic rocks from Sardinia, Corsica and Provence. N. Jb. Geol. Paläont., Mh. 1978 (1), 23–38.

Rong, J.Y., 1979. The Hirnantia fauna of China with comments on the Ordovician–Silurian boundary. Acta Stratigr. Sin. 3, 1–29 [in Chinese].

Rong, J.Y., Harper, D.A.T., 1988. A global synthesis of latest Ordovician Hirnantian brachiopod faunas. Trans. R. Soc. Edinburgh: Earth Sci. 79, 383–402.

Rosenbaum, G., Lister, G.S., Duboz, C., 2002. Relative motions of Africa, Iberia and Europe during Alpine orogeny. Tectonophysics 359, 117–129.

Rudnick, R.L., Gao, S., 2004. Composition of the Continental Crust. In: Holland, H.D., Turekian, K.K. (Eds.), Treatise on Geochemistry 3, 1–64. Elsevier, Amsterdam.

Schaltegger, U., Abrecht, J., Corfu, F., 2003. The Ordovician orogeny in the Alpine basement: constraints from geochronology and geochemistry in the Aar Massif (Central Alps). Schweiz. Miner. Petrol. Mitteil. 83, 183–195.

Schönlaub, H.P., 1998. Review of the Paleozoic paleogeography of the southern Alps – The perspective from the Austrian side. Giornale di Geologia 60, Spec. Iss., ECOS VII Southern Alps Field Trip Guidebook, 59–68.

Shaw, J., Johnston, S.T., Gutiérrez-Alonso, G., Weil, A.B., 2012. Oroclines of the Variscan orogeny of Iberia: paleocurrent analysis and paleogeographic implications. Earth Planet. Sci. Lett. 329–330, 60–70.

Shaw, J., Gutiérrez-Alonso, G., Johnston, S.T., Pastor Galán, D., Hofmann, M., 2014. Provenance variability along the Lower Ordovician north Gondwana margin: Paleogeographic and tectonic implications of U–Pb detrital zircon ages from the Armorican Quartzite of the Iberian Variscan belt. Geol. Soc. Am. Bull. 126, 702–719.

Sibuet, J.C., Srivastava, S.P., Sparkman, W., 2004. Pyrenean orogeny and plate kinematics. J. Geophys. Res. 109, B08104. doi:10.1029/2003JB002514.

Stampfli, G.M., Borel, G., 2002. A plate tectonic model for the Paleozoic and Mesozoic constrained by dynamic plate boundaries and restored synthetic oceanic isochrons. Earth Planet. Sci. Lett. 196, 17–33.

Stampfli, G.M., Von Raumer, J.F., Borel, G.D., 2002. Paleozoic evolution of pre–Variscan terranes: from Gondwana to the Variscan collision. In: Martínez Catalán, J.R., Hatcher, R.D., Arenas, R., Díaz García, F. (Eds.), Variscan–Appalachian Dynamics: The Building of the Late Paleozoic Basement. Geol. Soc. Am., Spec. Pap. 364, 263–280. Boulder, Colorado.

Stampfli, G.M., Hochard, C., Vérard, C., Wilhem, C., von Raumer, J.F., 2013. The geodynamics of Pangea formation. Tectonophysics 593, 1–19

Stille, H., 1939. Bemerkungen betreffend die "Sardische" Faltung und den Ausdruck "Ophiolitisch". Zeitschr. Deutsch. Geol. Ges. 91, 771–773.

Štorch, P., Feist, R., 2008. Lowermost Silurian graptolites of Montagne Noire, France. J. Paleont. 82, 938–956.

Sun, S.S., McDonough, W.H., 1989. Chemical and isotopic systematic of oceanic basalts: implications for mantle composition and processes. In: Saunders, A.D., Norry, M.J. (Eds.), Magmatism in the Ocean Basins. Geol. Soc., London, Spec. Pub. 42, 313–345.

Temple, J.T., 1965. Upper Ordovician brachiopods from Poland and Britain. Acta Palaeont. Polon. 10, 379–450.

Thoral, M., 1935. Contribution à l'étude géologique des Monts de Lacaune et des terrains cambriens et ordoviciens de la Montagne Noire. Librairie Polytechnique Ch. Béranger, Paris.

Touzeau, A., Lefebvre, B., Nardin, E., Gillard, M., 2012. Echinodermes de l'Ordovicien supérieur (Katien) des Corbières (Aude, France). Bull. Soc. Hist. Sci. Aude 112, 13–31.

Tugend, J., Manatschal, G., Kusznir, N.J., 2015. Spatial and temporal evolution of hyperextended rift systems: Implications for the nature, kinematics, and timing of the Iberian-European plate boundary. Geology 43, 15–18.

Vavrdová, M., 1966. Palaeozoic microplankton from central Bohemia. Èasopis pro Mineralogii a Geologii 11, 409–414.

Vila, J.M., 1965. Relations entre la nappe des Corbières orientales et son substratum dans la région de Durban-Corbières (Aude). C. R. Acad. Sci., Paris 260, 1700–1703.

Villas, E., 1985. Braquiópodos del Ordovícico medio y superior de las Cadenas Ibéricas Orientales. Mem. Mus. Paleont. Univ. Zaragoza 1, 1–153.

Villas, E., 1995. Caradoc through Early Ashgill brachiopods from the Central-Iberian zone (Central Spain). Geobios 28, 49–84.

Villas, E., Harper, D.A.T., Melou, M., Vizcaïno, D., 1995. Stratigraphical significance of the *Svobodaina* species (Brachiopoda, Heterorthidae) range in the Upper Ordovician of South-Western Europe, p. 97–98. In: Cooper, J.D., Droser, M.L., Finney, S.C. (Eds.), Ordovician

Odyssey. Short Papers for the seventh International Symposium on the Ordovician System, Las Vegas, USA.

Villas, E., Vennin, E., Álvaro, J.J., Hammann, W., Herrera, Z.A., Piovani, E.L., 2002. The late Ordovician carbonate sedimentation as a major triggering factor of the Hirnantian glaciation. Bull. Soc. géol. France 173, 569–578.

Vizcaïno, D., Álvaro, J.J. (Eds.), 2001. The Cambrian and Lower Ordovician of the southern Montagne Noire: a synthesis for the beginning of the new century. Ann. Soc. géol. Nord (2e sér.) 8, 185–242.

Vizcaïno, D., Álvaro, J.J., 2003. Adequacy of the Lower Ordovician trilobite record in the southern Montagne Noire (France): biases for biodiversity documentation. Trans. R. Soc. Edinburgh: Earth Sci. 93, 1–9.

Workman, R.K., Hart, S.R., 2005. Major and trace element composition of the depleted MORB mantle (DMM). Earth Planet. Sci. Lett. 231, 53–72.

Zurbriggen, R., 2015. Ordovician orogeny in the Alps: a reappraisal. Int. J. Earth Sci. 104, 335–350.

Zurbriggen, R., Franz, L., Handy, M.R., 1997. Pre–Variscan deformation, metamorphism and magmatism in the Strona-Ceneri Zone (southern Alps of northern Italy and southern Switzerland). Schweiz. Miner. Petrol. Mitteil. 77, 361–380.

FIGURE CAPTIONS

Figure 1. A. Major Variscan tectonostratigraphic units of SW Europe with location of the Montagne Noire and Mouthoumet massifs. B. Variscan nappes and thrust slices of the southern Montagne Nore and Mouthoumet massifs; study areas are coloured. Abbreviations: A-D: boxes in Figure 3, F: Faugères nappe, MN: Montagne Noire, Mo: Mouthoumet massif, MP: Mont Peyroux nappe, NPF: North Pyrenean Fault, SP: St. Pons nappe, VF: Villefrance (or Sillon Houiller) Fault.

Figure 2. Synthetic cross-section of the Montagne Noire with location of the Sardic unconformity; modified from Engel et al. (1980–1981) and Faure et al. (2004).

Figure 3. Geological sketches of the Cabrières klippes in the southern Montagne Noire and Mouthoumet study areas. A. Pre–Variscan outcrops in the vicinity of Neffiès, Cabrières klippes. B. Surroundings of Montjoi, Mouthoumet parautochthon. C. Davejean and Laroque de Fa, Félines-Palairac slice. D. Villerouge-Termenès, Félines-Palayrac slice. E. Legend; modified from Berger (1982), Bessière et al. (1984, 1989), Bessière and Baudelot (1988) and Berger et al.

(1990, 1993, 1997). Abbreviations- G: Gascagne stratotype, Ma: Marmairane stratotype, Mj: Montjoi stratotype, V: Villerouge stratotype. See Figure 1 for setting of mapped areas.

Figure 4. Stratigraphic framework of the Cambrian–Devonian strata and volcanic complexes in the southern Montagne Noire and Mouthoumet massif, with setting of representative stratigraphic gaps; based on Álvaro et al. (1998, 2014), Vizcaïno et al. (2001, 2003), and this work.

Figure 5. Schematic stratigraphic logs of the Lower Ordovician–Devonian in the southern Montagne Noire and Mouthoumet massif.

Figure 6. A. Ironstone composed of litharenitic sandstone cemented with iron oxyhydroxides bearing subrounded intraformational granules; basal part of Glauzy Formation at stratotype. B. Heterometric and polymictic conglomerate with litharenitic matrix and iron oxyhydroxide cement with subrounded clasts rich in authigenic glauconite (gl) and silicified shale (ss); basal part of Glauzy Formation at stratotype. C. Unsorted boulders embedded in a volcanosedimentary (litharenitic) matrix reflecting lahar deposits; top of Villerouge Formation at stratotype; D. Interbedded gravel litharenitic from the Villerouge Formation exhibiting flame-shaped lithic (silicified and partly ferruginized) clasts and strong welding foliation, at stratotype. E. Matrix of lahar deposit with silicified mosaics of former mafics embedded in a silicified matrix. F. Basal part of Gascagne Formation at stratotype exhibiting unsorted, polygenic, granule to very-coarse litharenite dominated by silicified shale clasts and subsidiary quartz, feldspar, chert, phantoms of mafic grains and iron oxyhydroxide clasts. G. Unsorted and polymictic granule litharenite rich in subrounded quartz, feldspar, chert and silicified mafics and shale clasts cemented with iron oxyhydroxide crusts, from the basal part of the Marmairane diamictite, along the road D212, Mouthoumet parautochthon. H. High-angle discordance of the subvertical Devonian (lower Geddinian) “mur quartzeux” (mq) and the subhorizontal Lower–Ordovician (Floian) Landeyran shales (Ls) close to the road along the Landeyran valley, Mt Peyroux nappe; scales (A, G) = 1mm, (B, D–F) = 2 mm, (C) 30 cm.

Figure 7. Representative fossils from the Gascagne Formation (A–I), Katian (Ka1–Ka2) in age, and from the Montjoi Formation (J–M), Katian (Ka2–Ka4) in age. A–D. *Kjaerina* (*Kjaerina*) *gondwanensis*, (A) latex cast of exterior of a ventral valve, MNHN.F.A53348; (B) internal mould of a ventral valve, MNHN.F.A53349; (C–D) latex cast of internal mould of a dorsal valve (C), MNHN.F.A53350, with detail of cardinalia (D) of an incomplete specimen, MNHN.F.A53351. E. *Rostricellula termieri*, internal mould of a dorsal valve, MNHN.F.A53352. F–G. *Portranella exornata*, (F) internal mould of a dorsal valve,

MNHN.F.A53353; (G) latex cast of exterior of a dorsal valve, MNHN.F.A53354. H. *Iberomena sardoa*, internal mould of a dorsal valve, MNHN.F.A53355. I. General aspect of a fossiliferous level showing several valves of the brachiopods *Svobodaina*? sp., *Drabovia* sp., a pygidium of the trilobite *Calymenella* cf. *boisseli*, "*Cornulites*" sp. and cystoid columnar plates, MNHN.F.A53356. J–K. *Nicolella actoniae*, internal mould (J), MNHN.F.A53357, and latex cast of exterior of a ventral valve (K) of a small specimen, MNHN.F.A53358. L. *Dolerorthis* sp., internal mould of an incomplete dorsal valve, MNHN.F.A53359. M. *Kjaerina* (*Villasina*) sp., latex cast of exterior of a ventral valve, MNHN.F.A53360. Fossils housed in the Muséum National d'Histoire Naturelle of Paris; all scales = 2 mm.

Figure 8. Brachiopods and trilobites from the Hirnantian Marmairane Formation. A–B. *Hirnantia sagittifera*, (A) internal mould of a dorsal valve, MNHN.F.A53361; and (B) internal mould of a ventral valve, MNHN.F.A53362. C–D. *Plectothyrella crassicosta* ssp., (C) internal mould of a ventral valve, MNHN.F.A53363; and (D) internal mould of a dorsal valve, MNHN.F.A53364. E. *Hindella crassa incipiens*, internal mould of a ventral valve, MNHN.F.A53365. F–G. *Leptaena trifidum*, (F) internal mould of a ventral valve, MNHN.F.A53366; and (G) internal mould of a dorsal valve, MNHN.F.A53367. H. *Eostropheodonta hirnantensis*, internal mould of a ventral valve, MNHN.F.A53368. I–J. *Kinnella kielanae*, (I) internal mould of a dorsal valve, MNHN.F.A53369; and (J) internal mould of a ventral valve, MNHN.F.A53370. K–L. *Flexicalymene* sp., cranidium and pygidium, external moulds; MNHN.F.A53371 and MNHN.F.A53372. M–N. *Mucronaspis* cf. *mucronata*, partial cephalon and pygidium, internal moulds; MNHN.F.A53373 and MNHN.F.A53374. O. Dalmanitid hypostome, internal mould, MNHN.F.A53375. P–R. *Lichas* sp., cephalon (latext cast of external mould) and pygidia (internal moulds), MNHN.F.A53376 and MNHN.F.A53377. Fossils housed in the Muséum National d'Histoire Naturelle of Paris; all scales = 2 mm.

Figure 9. Geochemical diagrams characterising the volcanic lava flows sampled in the Roque de Bandies and Villerouge formations A. N-MORB normalized incompatible element diagram; continental tholeiites (CT) average profile for comparison. B. Ti-Nb-Th diagram of Holm (1985) for distinguishing tholeiites from plate-margin initial rift tholeiites (IRT) and within-plate continental tholeiites (CT). C. Ta/Yb vs. Th/Yb diagram showing a Th enrichment that may be explained by crustal contamination due to incorporation of felsic xenoliths corresponding to the upper continental crust (UCC) composition. A moderately enriched source can be assumed; N-MORB normalizing values after Sun and McDonough (1989); continental tholeiite (CT) after Holm (1985); initial rift tholeiite (IRT) after Holm (1985) and Pouclet et al. (1995); PM, primitive mantle; N-MORB, E-MORB and OIB (oceanic island basalt)

compositions after Sun and McDonough (1989); depleted MORB mantle (DMM) after Workman and Hart (2005); upper continental crust (UCC) after Rudnick and Gao (2004).

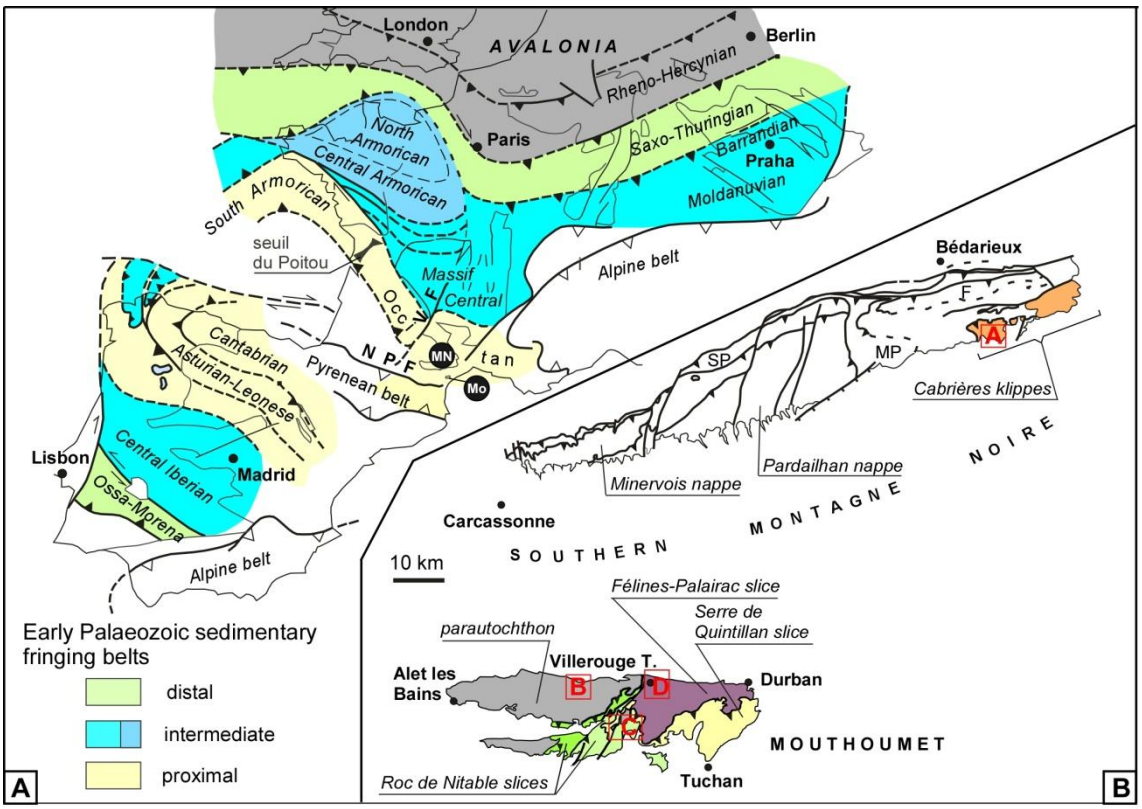

Figure 1. A. Major Variscan tectonostratigraphic units of SW Europe with location of the Montagne Noire and Mouthoumet massifs. B. Variscan nappes and thrust slices of the southern Montagne Nore and Mouthoumet massifs; study areas are coloured. Abbreviations: A-D: boxes in Figure 3, F: Faugères nappe, MN: Montagne Noire, Mo: Mouthoumet massif, MP: Mont Peyroux nappe, NPF: North Pyrenean Fault, SP: St. Pons nappe, VF: Villefrance (or Sillon Houiller) Fault.

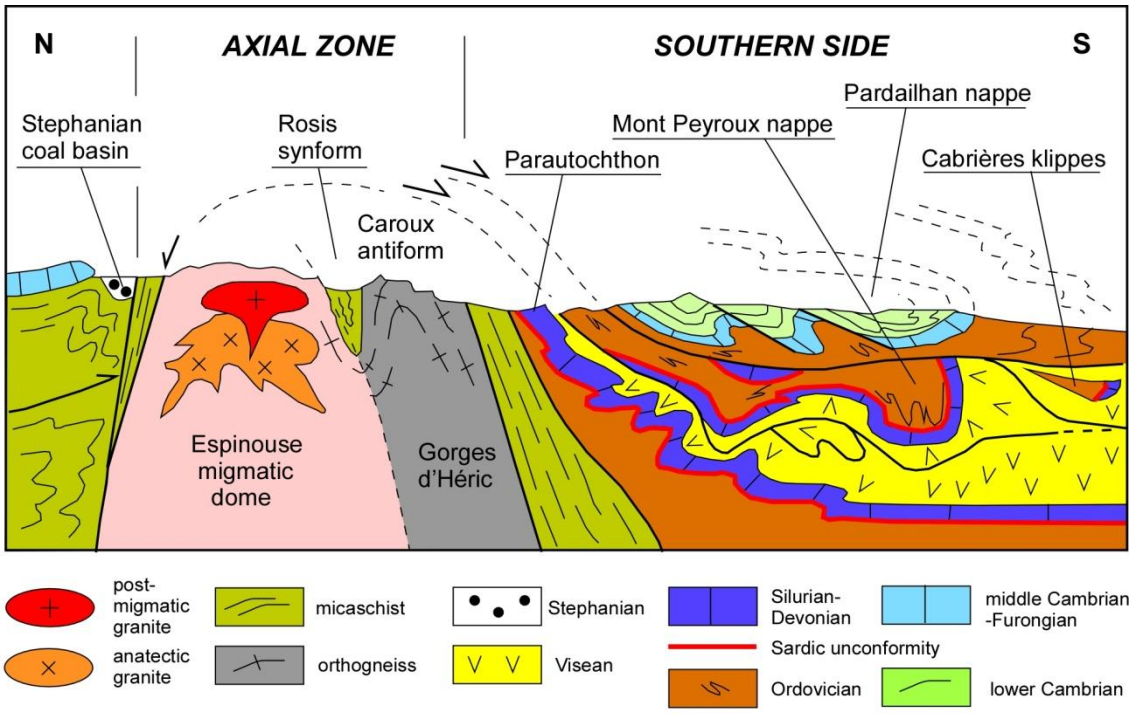

Figure 2. Synthetic cross-section of the Montagne Noire with location of the Sardic unconformity; modified from Engel et al. (1980–1981) and Faure et al. (2004).

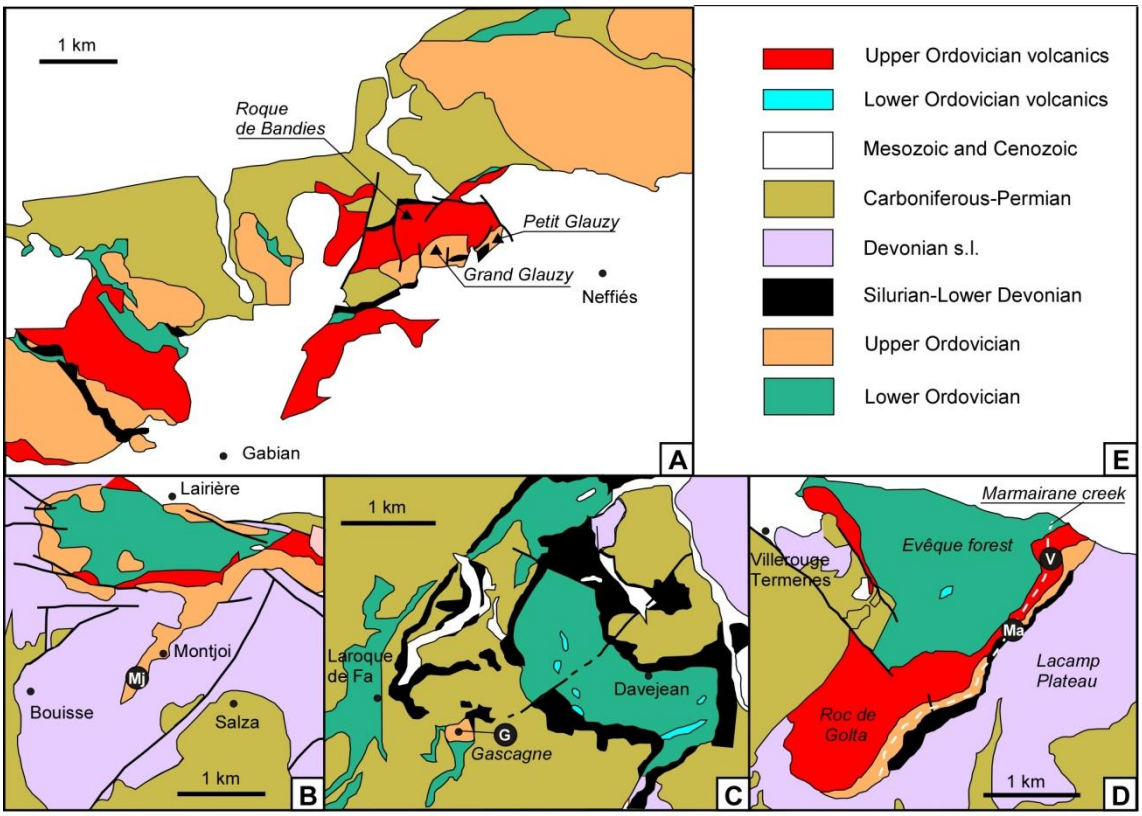

Figure 3. Geological sketches of the Cabrières klippes in the southern Montagne Noire and Mouthoumet study areas. A. Pre–Variscan outcrops in the vicinity of Neffiès, Cabrières klippes. B. Surroundings of Montjoi, Mouthoumet parautochthon. C. Davejean and Laroque de Fa, Félines-Palairac slice. D. Villerouge-Termenès, Félines-Palayrac slice. E. Legend; modified from Berger (1982), Bessière et al. (1984, 1989), Bessière and Baudelot (1988) and Berger et al. (1990, 1993, 1997). Abbreviations- G: Gascagne stratotype, Ma: Marmairane stratotype, Mj: Montjoi stratotype, V: Villerouge stratotype. See Figure 1 for setting of mapped areas.

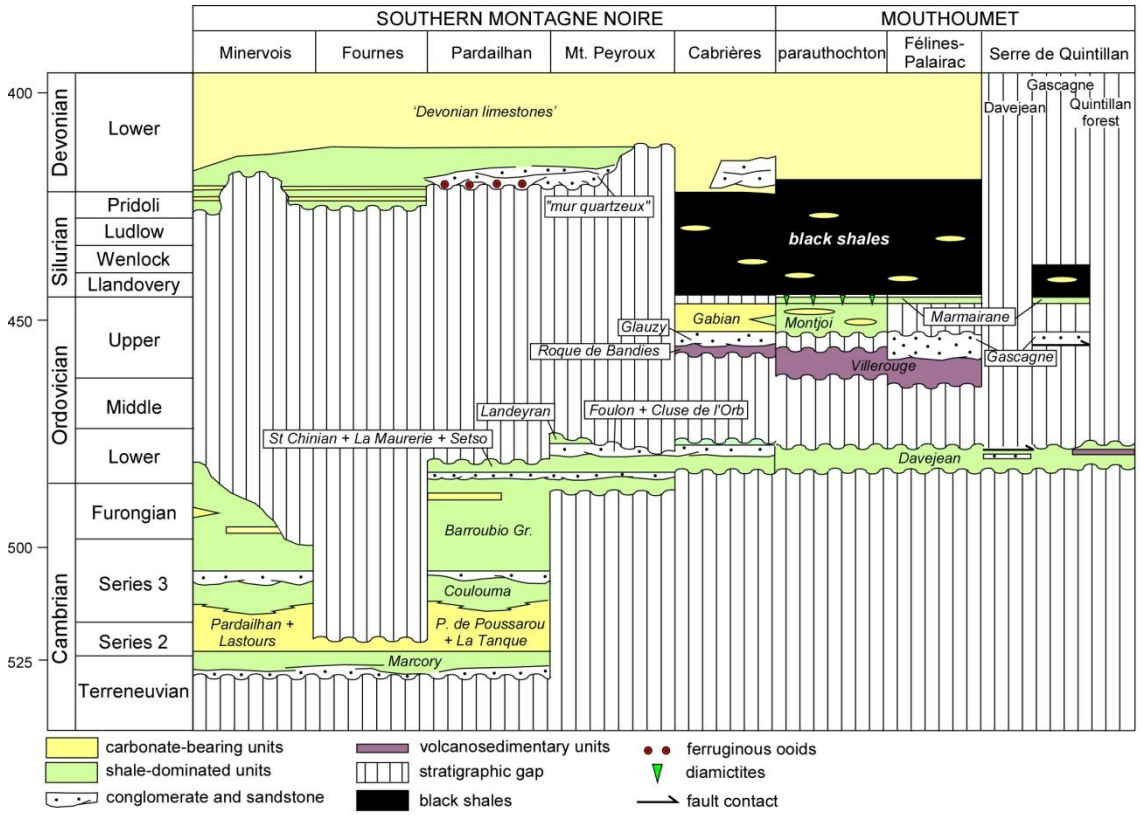

Figure 4. Stratigraphic framework of the Cambrian–Devonian strata and volcanic complexes in the southern Montagne Noire and Mouthoumet massif, with setting of representative stratigraphic gaps; based on Álvaro et al. (1998, 2014), Vizcaïno et al. (2001, 2003), and this work.

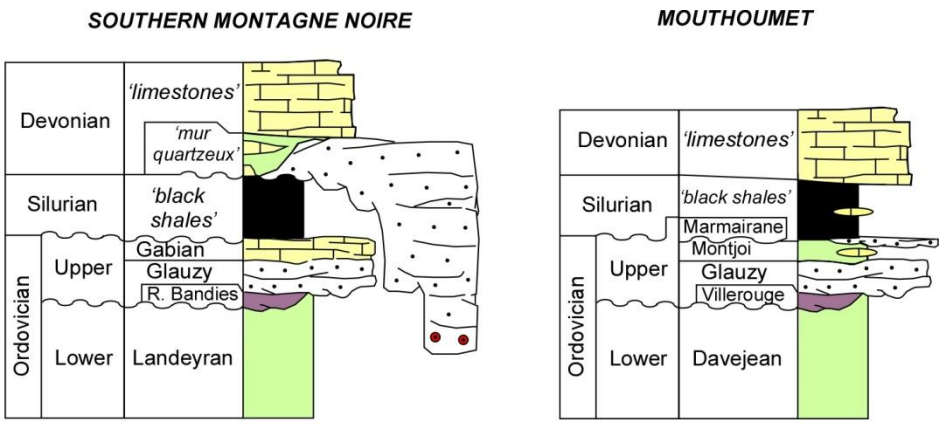

Figure 5. Schematic stratigraphic logs of the Lower Ordovician–Devonian in the southern Montagne Noire and Mouthoumet massif.

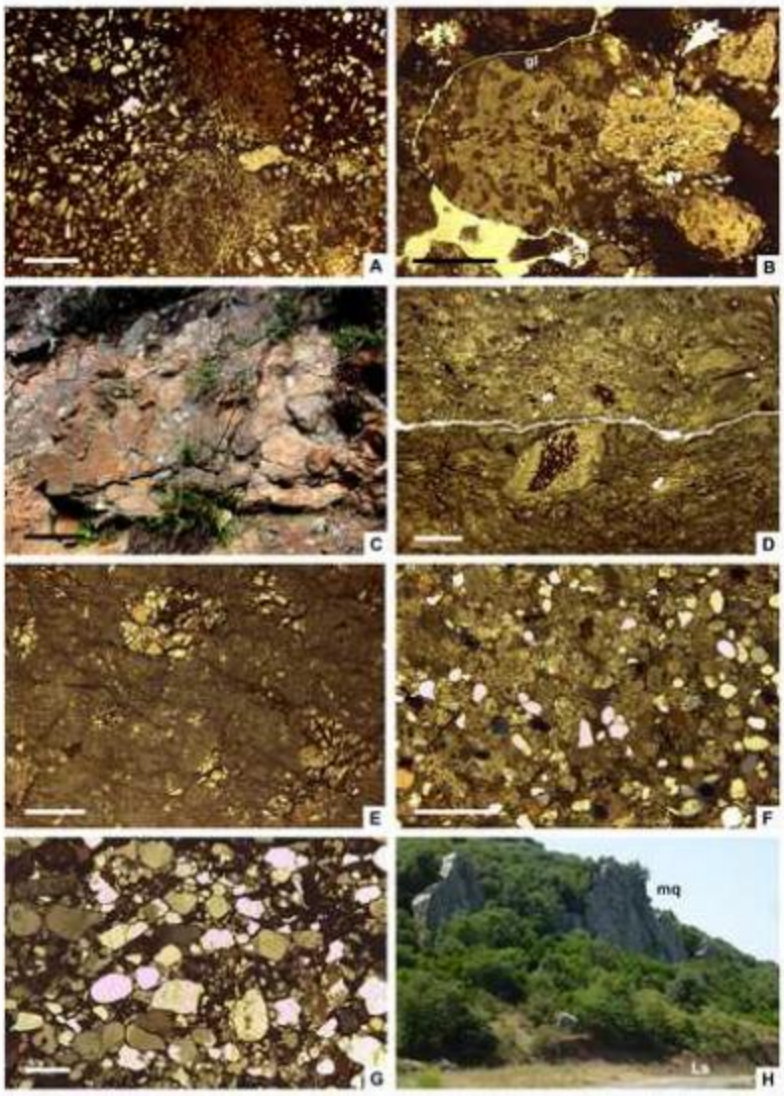

Figure 6

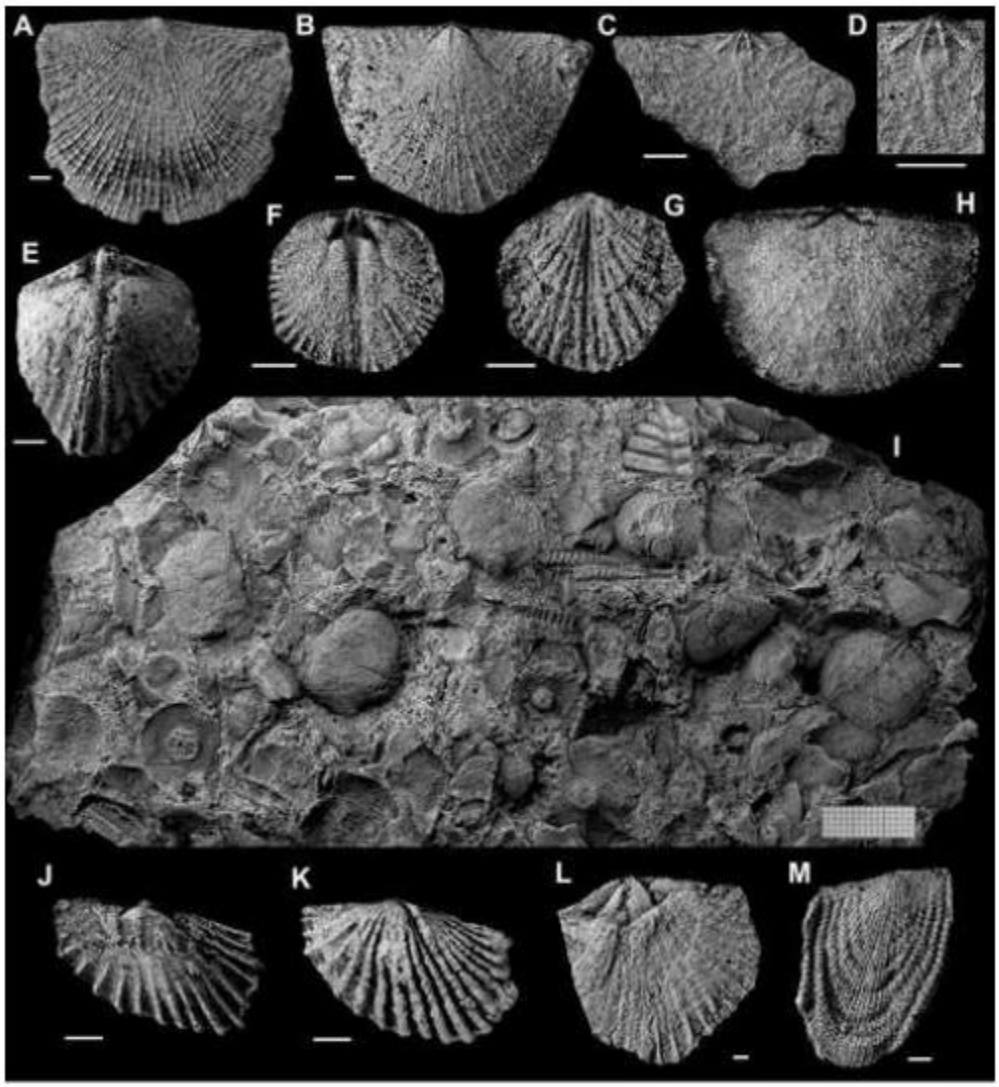

Figure 7

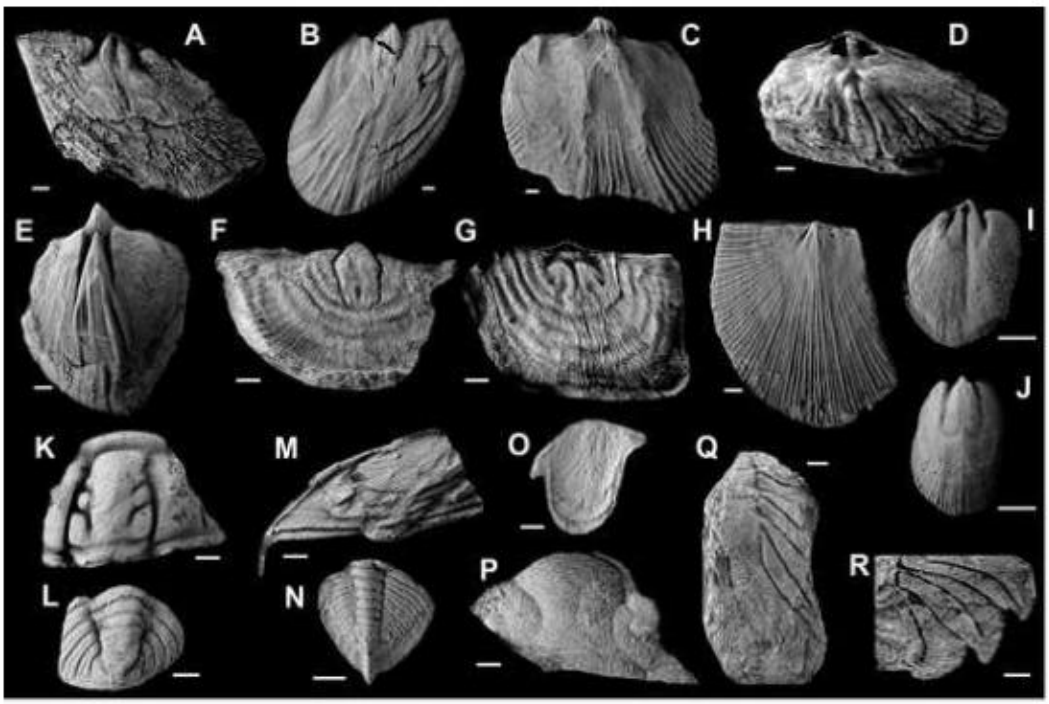

Figure 8

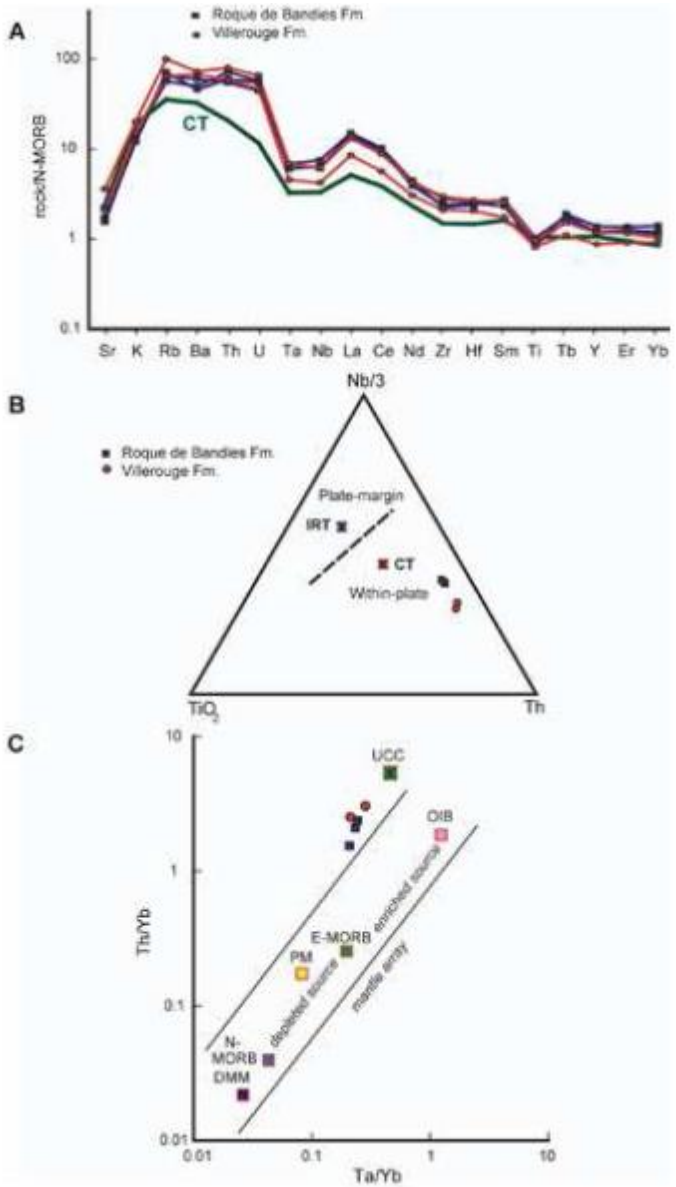

Figure 9

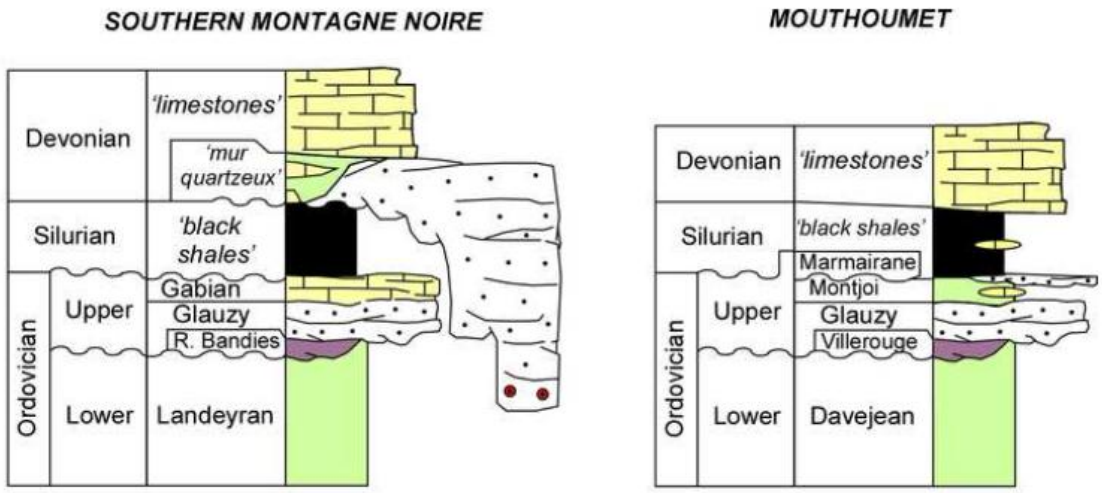

Schematic stratigraphic logs of the Lower Ordovician–Devonian in the southern Montagne Noire and Mouthoumet massif.

Graphical Abstract

Table 1. Chemical analyses of magmatic rocks. ICP and ICP-MS methods at ACME-LABS in Canada.

site	Roque de Bandies			Villerouge-Termenès	
#	GL-1a	GL-1f	GL-1b	VLR-14	VLR-2
major elements wt%					
SiO_2	53.12	54.15	58.35	57.11	58.29
TiO_2	1.06	1.09	1.3	1.22	1.04
Al_2O_3	14.52	14.95	16.95	18.71	17.89
Fe_2O_3 t	11.63	11.62	6.23	7.84	9.05
MnO	0.19	0.16	0.11	0.01	0.15
MgO	1.89	1.87	1.86	2.43	1.78
CaO	5.33	4.69	3.22	2.60	1.50
Na_2O	3.12	3.29	4.07	4.56	5.23
K_2O	0.87	0.93	1.03	1.46	1.09
P_2O_5	0.36	0.26	0.31	0.26	0.17
Cr_2O_3	0.01	0.01	0.01	0.00	0.01
LOI	7.70	6.80	6.40	3.50	3.60
Total	99.80	99.82	99.84	99.70	99.80

minor elements ppm					
Sc	20	19	19	21	21
V	176	180	193	107	104
Cr	34.21	34.21	75.27	20.53	88.95
Co	23.7	22.7	16.0	20.2	17.2
Ni	15.1	14.6	9.7	13.4	29.6
Cu	19.8	12.0	17.1	4.3	21.3
Zn	125	120	71	95	134
Ga	20.1	20.8	18.0	19.5	17.2
Rb	36.1	40.3	31.8	60.5	36.3
Sr	154.5	140.0	200.8	323.2	184.9
Y	38.7	32.9	33.5	32.9	24.5
Zr	167.4	177.3	208.6	218.3	155.6
Nb	14.2	14.9	17.5	14.3	9.8
Cs	2.5	2.9	2.9	9.6	4.7
Ba	378	290	315	456	429
Hf	4.9	5.1	5.3	5.5	4.2
Ta	0.9	0.8	0.9	0.9	0.6
Pb	6.4	3.7	9.2	2.7	6.5
Th	6.6	7.2	8.7	9.6	7.1
U	2.1	2.6	2.7	3.1	2.2
La	34.40	35.10	37.70	32.90	21.40
Ce	73.50	73.10	76.80	66.20	42.50
Pr	8.20	7.73	8.68	7.98	5.37
Nd	32.50	28.40	32.20	31.40	22.30
Sm	7.07	6.11	7.09	6.85	4.56
Eu	2.11	1.83	1.71	1.57	1.09
Gd	7.01	6.16	6.60	6.15	4.79
Tb	1.27	1.06	1.19	1.02	0.74
Dy	6.47	5.42	6.16	6.16	4.52
Ho	1.56	1.28	1.31	1.25	0.95
Er	4.05	3.70	3.72	3.44	2.70
Tm	0.69	0.59	0.57	0.50	0.37
Yb	4.29	3.42	3.66	3.15	2.82
Lu	0.69	0.61	0.52	0.50	0.36